bioRxiv preprint doi: https://doi.org/10.1101/2022.12.01.518799; this version posted December 2, 2022. The copyright holder for this preprint (which was not certified by peer review) is the author/funder, who has granted bioRxiv a license to display the preprint in perpetuity. It is made available under aCC-BY-NC-ND 4.0 International license.

Characterization of the Human Immunodeficiency Virus (HIV-1) Envelope Glycoprotein Conformational States on Infectious Virus Particles

Hanh T. Nguyen[a,b,*], Qian Wang[a,b], Saumya Anang[a,b] and Joseph G. Sodroski[a,b,*]

[a]Department of Cancer Immunology and Virology, Dana-Farber Cancer Institute, Boston, MA 02215, USA

[b]Department of Microbiology, Harvard Medical School, Boston, MA 02215, USA

*Corresponding authors:
Hanh T. Nguyen, Ph.D.
Joseph G. Sodroski, M.D.
Dana-Farber Cancer Institute
450 Brookline Avenue, CLS 1010
Boston, MA 02215
Phone: 617-632-3371 Fax: 617-632-4338
Email: hanht_nguyen@dfci.harvard.edu, joseph_sodroski@dfci.harvard.edu

Running title: HIV-1 Env Conformations on Virus Particles

Abstract word count: 250

bioRxiv preprint doi: https://doi.org/10.1101/2022.12.01.518799; this version posted December 2, 2022. The copyright holder for this preprint (which was not certified by peer review) is the author/funder, who has granted bioRxiv a license to display the preprint in perpetuity. It is made available under aCC-BY-NC-ND 4.0 International license.

ABSTRACT

Human immunodeficiency virus (HIV-1) entry into cells involves triggering of the viral envelope glycoprotein (Env) trimer ($(gp120/gp41)_3$) by the primary receptor, CD4, and coreceptors, CCR5 or CXCR4. The pretriggered (State-1) conformation of the mature (cleaved) Env is targeted by broadly neutralizing antibodies (bNAbs), which are inefficiently elicited compared with poorly neutralizing antibodies (pNAbs). Here we characterize variants of the moderately triggerable HIV-1_{AD8} Env on virions produced by an infectious molecular proviral clone; such virions contain more cleaved Env than pseudotyped viruses. We identified three types of cleaved wild-type AD8 Env trimers on virions: 1) State-1-like trimers preferentially recognized by bNAbs and exhibiting strong subunit association; 2) trimers recognized by pNAbs directed against the gp120 coreceptor-binding region and exhibiting weak, detergent-sensitive subunit association; and 3) a minor gp41-only population. The first Env population was enriched and the other Env populations reduced by introducing State-1-stabilizing changes in the AD8 Env or by treatment of the virions with crosslinker or the State-1-preferring entry inhibitor, BMS-806. These stabilized AD8 Envs were also more resistant to gp120 shedding induced by a CD4-mimetic compound or by incubation on ice. Conversely, a State-1-destabilized, CD4-independent AD8 Env variant exhibited weaker bNAb recognition and stronger pNAb recognition. Similar relationships between Env triggerability and antigenicity/shedding propensity on virions were observed for other HIV-1 strains. Our results show that State-1 Envs on virions can be significantly enriched by optimizing Env cleavage; stabilizing the pretriggered conformation by Env modification, crosslinking or BMS-806 treatment; strengthening Env subunit interactions; and using CD4-negative producer cells.

bioRxiv preprint doi: https://doi.org/10.1101/2022.12.01.518799; this version posted December 2, 2022. The copyright holder for this preprint (which was not certified by peer review) is the author/funder, who has granted bioRxiv a license to display the preprint in perpetuity. It is made available under aCC-BY-NC-ND 4.0 International license.

IMPORTANCE

Efforts to develop an effective HIV-1 vaccine have been frustrated by the inability to elicit broad neutralizing antibodies that recognize multiple virus strains. Such antibodies are able to bind a particular shape of the HIV-1 envelope glycoprotein trimer, as it exists on a viral membrane but before engaging receptors on the host cell. Here, we establish simple yet powerful assays to characterize the envelope glycoproteins in a natural context on virus particles. We find that, depending on the HIV-1 strain, some envelope glycoproteins change shape and fall apart, creating decoys that can potentially divert the host immune response. We identify requirements to keep the relevant envelope glycoprotein target for broad neutralizing antibodies intact on virus-like particles. These studies suggest strategies that should facilitate efforts to produce and use virus-like particles as vaccine immunogens.

KEYWORDS: membrane Env, native conformation, pretriggered conformation, State 1, stabilizing mutation, infectious molecular clone, provirus, virus-like particle, immunogen, vaccine

bioRxiv preprint doi: https://doi.org/10.1101/2022.12.01.518799; this version posted December 2, 2022. The copyright holder for this preprint (which was not certified by peer review) is the author/funder, who has granted bioRxiv a license to display the preprint in perpetuity. It is made available under aCC-BY-NC-ND 4.0 International license.

INTRODUCTION

Human immunodeficiency virus type 1 (HIV-1) entry into target cells is mediated by the viral envelope glycoprotein (Env) trimer, which is composed of three gp120 exterior subunits and three gp41 transmembrane subunits (1,2). In infected cells, Env is synthesized as an uncleaved precursor in the rough endoplasmic reticulum (ER), where signal peptide cleavage, folding, trimerization, and the addition of high-mannose glycans take place (3-6). Exiting the ER, the trimeric gp160 Env precursor follows two pathways to the cell surface (7). In the conventional secretory pathway, the Env precursor transits through the Golgi compartment, where it is cleaved into gp120 and gp41 subunits and is further modified by the addition of complex sugars (8-11). These mature Envs are transported to the cell surface and are incorporated into virions (7). In the second pathway, the gp160 precursor bypasses the Golgi compartment and traffics directly to the cell surface; these uncleaved gp160 Envs lack complex carbohydrates and are excluded from virions (7).

Single-molecule fluorescence resonance energy transfer (smFRET) experiments indicate that, on virus particles, the Env trimer exists in three conformational states (States 1 to 3) (12). From its pretriggered conformation (State 1), the metastable Env trimer interacts with the receptors, CD4 and CCR5 or CXCR4, and undergoes transitions to lower-energy states (13-16). Initially, the engagement with CD4 induces an asymmetric intermediate Env conformation, with the CD4-bound protomer in State 3 and the unliganded protomers in State 2 (17). Binding of additional CD4 molecules to the Env trimer then induces the full CD4-bound, prehairpin intermediate conformation, with all three Env protomers in State 3 (12,17). An extended coiled coil consisting of the

bioRxiv preprint doi: https://doi.org/10.1101/2022.12.01.518799; this version posted December 2, 2022. The copyright holder for this preprint (which was not certified by peer review) is the author/funder, who has granted bioRxiv a license to display the preprint in perpetuity. It is made available under aCC-BY-NC-ND 4.0 International license.

heptad repeat (HR1) region of gp41 is exposed in the prehairpin intermediate (18-21). State-3 Env protomers subsequently interact with CCR5 or CXCR4 coreceptors to trigger the formation of a gp41 six-helix bundle, a process that results in fusion of the viral and target cell membranes (22-26).

Env is the only virus-specific molecule exposed on the viral surface and thus represents the major target for host neutralizing antibodies (27-29). Env strain variability, heavy glycosylation, conformational flexibility and structural heterogeneity are thought to contribute to HIV-1 persistence by diminishing the elicitation and binding of neutralizing antibodies (27-32). During natural infection, high titers of antibodies are elicited that recognize the gp160 Env precursor, which samples multiple conformations, and disassembled Envs (shed gp120, gp41 six-helix bundles) (33-45). These antibodies are poorly neutralizing because they fail to recognize the mature functional Env trimer, which mainly resides in State 1 (12,36,38,41-49). After years of infection, some HIV-1-infected individuals generate broadly neutralizing antibodies (bNAbs), most of which recognize the pretriggered (State-1) Env conformation (12,46-58). Passively administered monoclonal bNAbs are protective in animal models of HIV-1 infection, suggesting that the elicitation of bNAbs is an important goal for vaccines (59-63). Unfortunately, bNAbs have not been efficiently and consistently elicited in animals immunized with current vaccine candidates, including stabilized soluble gp140 (sgp140) SOSIP.664 trimers (64-75). Soluble Env trimers often elicit strong strain-restricted neutralizing antibodies or poorly neutralizing antibodies (pNAbs) targeting the gp120 V3 variable loop, neo-epitopes at the base of the trimer, or holes in the glycan shield (68,76-84).

bioRxiv preprint doi: https://doi.org/10.1101/2022.12.01.518799; this version posted December 2, 2022. The copyright holder for this preprint (which was not certified by peer review) is the author/funder, who has granted bioRxiv a license to display the preprint in perpetuity. It is made available under aCC-BY-NC-ND 4.0 International license.

Differences in the antigenicity, glycosylation and conformation of sgp140 SOSIP.664 trimers and the pretriggered (State-1) membrane Env have been observed (11,85-96). Given the requirement for bNAbs to recognize conserved and conformationally-specific elements on the pretriggered (State-1) Env (12,46-49), even small differences from the native State-1 Env might affect immunogen efficacy. First, differences in the composition of the glycan shield of sgp140 SOSIP.664 trimers and membrane Env (11,90-93) could hamper the elicitation of bNAbs, most of which recognize epitopes that include glycan components or are surrounded by glycans that influence antibody access (28,29,32,97-101). Currently, the only way to obtain a glycan shield resembling that of the virion Env spike is to produce the Env trimer immunogen in a membrane-anchored form. Second, membrane Env trimer immunogens also have the capacity to present the full set of quaternary bNAb epitopes (including the gp41 membrane-proximal external region (MPER)) to the immune system. Although the MPER is important for the maintenance of the State-1 Env conformation (102-113), the MPER is removed from sgp140 SOSIP.664 trimers to prevent aggregation (32,114-117). Finally, immunodominant responses against neo-epitopes artefactually created in the base of soluble timers (79,84) could be eliminated by using membrane Env trimer immunogens. Overall, these considerations indicate that a membrane Env immunogen may have considerable advantages in presenting a native State-1 Env conformation to the host immune system.

Virus-like particles (VLPs) are an attractive platform for HIV-1 membrane Env immunogens, as virions represent a natural environment for the functional Env trimer

bioRxiv preprint doi: https://doi.org/10.1101/2022.12.01.518799; this version posted December 2, 2022. The copyright holder for this preprint (which was not certified by peer review) is the author/funder, who has granted bioRxiv a license to display the preprint in perpetuity. It is made available under aCC-BY-NC-ND 4.0 International license.

and should accurately reproduce the relevant bNAb target. The relative enrichment of Golgi-passaged Env in virions and VLPs results in Env trimers that are cleaved, authentically glycosylated and imbedded in a cholesterol/sphingomyelin-rich (lipid raft-like) membrane, all of which are conducive to the maintenance of a pretriggered (State-1) conformation (40-45,107-113,118). Although the low Env content of VLPs (mimicking the natural 10-14 Env spikes per virion (119,120)) is not an absolute barrier to their use as immunogens, methods for efficient VLP production must be optimized. Of potentially greater importance is the quality of the Env on VLPs; indeed, several studies have documented significant Env heterogeneity in VLP preparations (121-137). Proteolytically mature Env is enriched in virions produced by infected cells; however, systems overexpressing HIV-1 Gag and Env often produce VLPs with significant levels of uncleaved Env (7,124-127,134,137). Uncleaved Env, which is flexible and prone to assume non-State-1 conformations recognizable by pNAbs (40-45), is a highly undesirable contaminant in any immunogen attempting to focus the host antibody response on the pretriggered (State-1) Env conformation. Envs with disrupted subunit interactions, manifest in the extreme case by shedding of gp120 from the trimer, represent other potential sources of heterogeneity (137-139).

Here, we study Env conformation on infectious HIV-1 particles, examining both cleaved and uncleaved Env populations. We compare viral pseudotypes and virions produced by infectious molecular proviral clones (IMCs). We evaluate the antigenicity and propensity to shed gp120 for Envs from different HIV-1 strains and Envs modified to stabilize distinct conformational states. These studies provide useful assays and

bioRxiv preprint doi: https://doi.org/10.1101/2022.12.01.518799; this version posted December 2, 2022. The copyright holder for this preprint (which was not certified by peer review) is the author/funder, who has granted bioRxiv a license to display the preprint in perpetuity. It is made available under aCC-BY-NC-ND 4.0 International license.

reagents for the study of Env in a natural membrane context and can guide the optimization of Env quality in VLPs.

RESULTS

Comparison of systems transiently expressing virus particles.

To identify a virus-producing system that could yield sufficient levels of cleaved Env for detailed analysis, we compared 293T cells transiently expressing either pseudotyped viruses or virions produced by an infectious molecular proviral clone (IMC). Viruses pseudotyped by the tier-2 primary HIV-1_{AD8} Env were produced by cotransfection of a plasmid expressing the AD8 Env and an *env*-negative provirus vector, pNL4-3.ΔEnv (originally pNL4-3.Luc.R-E- from the NIH HIV Reagent Program). In the pNL4-3.AD8 IMC, the NL4-3 *env* gene was replaced by that of AD8. The AD8 Envs produced by both expression systems have a signal peptide and C-terminal gp41 cytoplasmic tail from HXBc2/NL4-3 Envs. As seen in Fig. 1A, pseudotyped virus particles contained mostly uncleaved Env with little cleaved Env. By contrast, virions produced by the IMC incorporated at least as much Env per particle, but with ~5.7-fold more gp120 relative to gp160. The pNL4-3.AD8 IMC also produced virions with efficiently cleaved Env in HeLa cells (Fig. 1A). Varying the transfected amounts of the Env-expressing and *env*-negative proviral plasmids failed to increase the gp120:gp160 ratio of the pseudovirus particles to a level comparable to that of the IMC-produced virions (Fig. 1B). These observations indicated that the IMC system could produce virus particles with sufficient quantities of cleaved Env for our study.

bioRxiv preprint doi: https://doi.org/10.1101/2022.12.01.518799; this version posted December 2, 2022. The copyright holder for this preprint (which was not certified by peer review) is the author/funder, who has granted bioRxiv a license to display the preprint in perpetuity. It is made available under aCC-BY-NC-ND 4.0 International license.

Next, we examined the effects of Env cleavage and cytoplasmic tail truncation on the quantity and quality of Env on virions produced by an IMC. Although the cleavage-defective AD8 Env was expressed well in the IMC-transfected cells, the uncleaved Env was incorporated into virions less efficiently than the cleavage-competent AD8 Env (Fig. 1C). Complete truncation of the Env cytoplasmic tail at residue 712 did not affect the gp120:gp160 ratio on virions, but slightly increased the level of cleaved Env incorporated.

To evaluate whether HIV-1 proteins that are not required for virion production affect Env incorporation, we individually knocked out the expression of reverse transcriptase (RT), RNAse H, integrase (IN), Vif, Vpr, Vpu and Nef (Fig. 1D). None of these knockouts affected the level of Env incorporation into VLPs or Env cleavage on the VLPs. As expected (140-142), the infectivity of the virus particles was dramatically reduced by the introduction of stop codons in the RT, RNAse H and IN open reading frames.

Characterization of the AD8 Env on virus particles.

Having established the suitability of the IMC expression system for producing VLPs, we characterized the AD8 Env on the virus particles. Deglycosylation with PNGase F and Endoglycosidase Hf demonstrated that all the cleaved Env on virus particles is modified by complex glycans; some of the gp160 glycoprotein on virus particles is also modified by complex carbohydrates (Fig. 2A). Therefore, all the cleaved Env and some of the uncleaved Env on these virus particle preparations has passed through the Golgi network (7). Interestingly, we observed two distinct bands for the

bioRxiv preprint doi: https://doi.org/10.1101/2022.12.01.518799; this version posted December 2, 2022. The copyright holder for this preprint (which was not certified by peer review) is the author/funder, who has granted bioRxiv a license to display the preprint in perpetuity. It is made available under aCC-BY-NC-ND 4.0 International license.

deglycosylated gp160 and gp41 proteins, indicating the presence of truncated forms of these Envs. In parallel studies, we determined that clipping of the Env cytoplasmic tail at Arg 747 by the viral protease generates these truncated gp160 and gp41 proteins in the virus particles, a phenomenon that has been previously reported (143,144). This protease-mediated clipping is enhanced by changes introduced into the AD8 Env cytoplasmic tail (F752S and F756I) as a result of the chimeric AD8-NL4-3 Env junction (at the BamHI site of *env*). Reverting these two cytoplasmic tail changes to the phenylalanine residues at 752 and 756 found in the wild-type HIV-1_{AD8} Env minimizes cytoplasmic tail clipping in the virus particles (see below). The AD8 Env containing Phe 752 and Phe 756, herein designated AD8 Bam, serves as the "wild-type" Env in this study.

To examine the oligomeric composition of the AD8 Bam Envs on virions, purified virus particles were incubated with the crosslinker bis(sulfosuccinimidyl)suberate (BS3). As the BS3 concentration was increased, the AD8 Bam Env was efficiently crosslinked into gel-stable trimers, with no higher-molecular-weight forms observed (Fig. 2B). We conclude that essentially all the AD8 Bam Envs on these virus particles are assembled into trimers.

To examine the antigenicity of the AD8 Bam Env on virus particles, an immunoprecipitation assay was performed with a panel of broadly neutralizing antibodies (bNAbs) and poorly neutralizing antibodies (pNAbs) targeting the gp120 and gp41 glycoproteins. The bNAbs included 2G12 against gp120 outer-domain glycans (145), VRC03 against the gp120 CD4-binding site (CD4BS) (146), PG16 and PGT145

bioRxiv preprint doi: https://doi.org/10.1101/2022.12.01.518799; this version posted December 2, 2022. The copyright holder for this preprint (which was not certified by peer review) is the author/funder, who has granted bioRxiv a license to display the preprint in perpetuity. It is made available under aCC-BY-NC-ND 4.0 International license.

against quaternary gp120 epitopes at the trimer apex (147,148), PGT151 and 35O22 against the gp120-gp41 interface (149,150), and 10E8.v4 against the gp41 membrane-proximal external region (MPER) (106). The pNAbs included 19b and 447-52D, 3074, 3869 and 39F against the gp120 V3 region (151,152), 17b and E51 against gp120 CD4-induced (CD4i) epitopes (153,154), F105 against the gp120 CD4BS (155,156), 902090 against the gp120 V2 region (157), and F240 against a Cluster I epitope on gp41 (158). C34-Ig is a fusion protein consisting of an immunoglobulin heavy chain and a gp41 HR2 peptide, C34, that targets the gp41 HR1 coiled coil (21). In the antigenicity assay performed in the absence of the soluble CD4 (sCD4) receptor, 2G12 precipitated both uncleaved and cleaved Envs, whereas the other bNAbs preferentially recognized the cleaved Envs (Fig. 2C, −sCD4 panels). All the bNAbs efficiently precipitated both gp120 and gp41 subunits, indicating that the subunits of the AD8 Bam Env trimers recognized by bNAbs remain associated during detergent solubilization, immunoprecipitation and washing of the immunoprecipitates. The pNAbs recognized the uncleaved gp160 Env, as expected (38,39). The pNAbs against the gp120 V3 region and CD4i epitopes also precipitated the gp120 subunit of the cleaved AD8 Bam Env with surprising efficiency. Of interest, these pNAbs (19b, 447-52D and 17b) coprecipitated gp41 less efficiently than the gp120-directed bNAbs. The F240 antibody and C34-Ig recognized gp41 but did not coprecipitate gp120; these ligands are presumably recognizing gp41 glycoproteins that are not stably associated with gp120.

Together these observations suggest that the unliganded AD8 Bam Env on virus particles was processed in the Golgi apparatus and forms trimers with the following antigenic properties: (i) the uncleaved Env could be recognized by pNAbs, consistent

bioRxiv preprint doi: https://doi.org/10.1101/2022.12.01.518799; this version posted December 2, 2022. The copyright holder for this preprint (which was not certified by peer review) is the author/funder, who has granted bioRxiv a license to display the preprint in perpetuity. It is made available under aCC-BY-NC-ND 4.0 International license.

with its conformational flexibility (39-45); (ii) the cleaved Envs could be recognized by bNAbs and some V3- and CD4i-directed pNAbs, which recognize gp120 structures involved in coreceptor binding (151-154,159,160); and (iii) the cleaved Envs that are recognized by bNAbs exhibit stronger gp120-trimer association in detergent than those that are recognized by pNAbs, suggesting differences in conformation between the two cleaved Env populations.

To examine the effects of receptor binding on the conformation of the AD8 Bam Env on virus particles, we performed the antigenicity assay in the presence of soluble four-domain CD4. In these experiments, we utilized conditions that were predetermined to allow detection of Env conformational changes with only minimal shedding of gp120 (data not shown). Incubation with sCD4 led to a significant increase in the binding of V3- and CD4i-directed pNAb binding to gp120; this was not accompanied by an increase in gp41 precipitation for the 19b, 447-52D and 17b pNAbs (Fig. 2C, +sCD4 panels). The E51 CD4i pNAb precipitated more gp120 and gp41 in the presence of sCD4, suggesting that complexes of the AD8 Bam Env, sCD4 and E51 antibody remain associated throughout detergent solubilization and washing. Mild increases in gp41 recognition by F240 and C34-Ig were also observed following incubation with sCD4, consistent with sCD4-induced shedding of gp120 from the Env trimers (161).

The small-molecule HIV-1 entry inhibitor, BMS-806, has been suggested to stabilize a pretriggered (State-1) conformation in membrane Envs (12,21,38,95,118,162,163). Chemical crosslinkers like

bioRxiv preprint doi: https://doi.org/10.1101/2022.12.01.518799; this version posted December 2, 2022. The copyright holder for this preprint (which was not certified by peer review) is the author/funder, who has granted bioRxiv a license to display the preprint in perpetuity. It is made available under aCC-BY-NC-ND 4.0 International license.

3,3'-dithiobis(sulfosuccinimidyl)propionate (DTSSP) are often used to limit the conformational dynamics of proteins (39). To examine the effects of these treatments on the conformation of the AD8 Bam Env on virus particles, we performed the immunoprecipitation assay in the presence of 10 μM BMS-806 or after crosslinking the viruses with 0.1 mM or 1 mM DTSSP (Fig. 2D). There were two significant differences in the antigenicity of Env on treated and untreated virus articles. First, both BMS-806 treatment or DTSSP crosslinking significantly reduced gp120 recognition by pNAbs. Crosslinking with 1 mM DTSSP did not affect pNAb binding to soluble gp120 monomers (Fig. 2E), ruling out an effect of DTSSP on the pNAb epitopes *per se* and indicating the importance of the Env trimer context to the observed reduction in pNAb binding. The results are consistent with BMS-806 and DTSSP treatment reducing spontaneous Env transitions from a pretriggered (State-1) conformation to more open downstream conformations recognizable by V3 and CD4i pNAbs. Second, treatment with the higher concentration of DTSSP led to a reduction in the binding of the PG16 and PGT145 bNAbs, which recognize V2 quaternary structures at the trimer apex (92,147,148,164). The binding of these bNAbs was not decreased by treatment with BMS-806 or lower concentrations of DTSSP. The observed reduction in PG16 and PGT145 bNAb binding after treatment with higher DTSSP concentrations may result from modification of key gp120 lysine residues shown to be important for the binding of these antibodies (92,164).

Effects of cytoplasmic tail clipping on Env conformation.

As mentioned above, clipping of the AD8 Env cytoplasmic tail by the HIV-1 protease is enhanced by the alteration of two phenylalanine residues (Phe 752 and Phe

bioRxiv preprint doi: https://doi.org/10.1101/2022.12.01.518799; this version posted December 2, 2022. The copyright holder for this preprint (which was not certified by peer review) is the author/funder, who has granted bioRxiv a license to display the preprint in perpetuity. It is made available under aCC-BY-NC-ND 4.0 International license.

309 756) near the cleavage site (our unpublished observations). To evaluate the effect of
310 cytoplasmic tail clipping on Env conformation, we compared the AD8 Env with the AD8
311 Bam Env, in which the S752F + I756F reversions were introduced. Little gp160 or gp41
312 clipping was detected in the lysates of cells expressing the AD8 and AD8 Bam Envs
313 (Fig. 3A), consistent with this clipping being mediated by the HIV-1 protease, which is
314 activated by dimerization in virion particles (165). On virus particles, approximately 72%
315 of the AD8 gp41 was clipped, whereas only 28% of the AD8 Bam gp41 was clipped
316 (Fig. 3A). Despite these differences in the level of clipped gp41, no significant
317 differences were observed in the sensitivity of the AD8 and AD8 Bam viruses to
318 neutralization by bNAbs, pNAbs, sCD4-Ig or BNM-III-170, a CD4-mimetic compound
319 (CD4mc) (166) (Fig. 3B). The qualitative pattern of bNAb and pNAb binding to the AD8
320 and AD8 Bam virus particles was similar (Fig. 3C). The AD8 Env conformation and
321 neutralization sensitivity are not apparently affected by protease-mediated gp41 clipping
322 in virions.
323
324 **Effects of State-1-stabilizing and -destabilizing changes on virion Env.**
325 Previous studies have identified HIV-1 Env variants in which the pretriggered
326 (State-1) conformation is stabilized, rendering the viruses more resistant to cold
327 inactivation and to inhibition by sCD4 and the CD4mc BNM-III-170 (167). Conversely,
328 Env variants in which State 1 is destabilized often exhibit global increases in sensitivity
329 to inactivation at 0^{o} C and to neutralization by sCD4, CD4mcs and pNAbs (107-
330 113,168-169). To evaluate the effect of State-1-stabilizing and -destabilizing changes on
331 the antigenicity of Env on viruses, we introduced these changes into the AD8 Bam Env.
332 Three changes (Q114E, Q576K and A582T) critical to the State-1-stabilized phenotype

bioRxiv preprint doi: https://doi.org/10.1101/2022.12.01.518799; this version posted December 2, 2022. The copyright holder for this preprint (which was not certified by peer review) is the author/funder, who has granted bioRxiv a license to display the preprint in perpetuity. It is made available under aCC-BY-NC-ND 4.0 International license.

of a previously reported HIV-1_{AD8} Env variant, AE.2 (167), were introduced into the AD8 Bam Env to create the Tri Bam Env. Multiple Env polymorphisms found in the AE.2 Env, including the State-1-stabilizing A114E, Q567K and A582T changes, were introduced into the AD8 Bam Env to create the AE.1 Bam Env (see Materials and Methods for details). The sensitivity of viruses with the AD8 Bam, Tri Bam and AE.1 Bam Envs to inhibition by sCD4-Ig and the CD4mc BNM-III-170 was measured using TZM-bl target cells. The sCD4-Ig IC_{50} values were 0.076 (AD8 Bam), >20 (Tri Bam) and >20 (AE.1 Bam) μg/ml. The BNM-III-170 IC_{50} values were 0.22 (AD8 Bam), >100 (Tri Bam) and >100 (AE.1 Bam) μM. The viruses with the Tri Bam and AE.1 Bam Envs were also more resistant to inactivation on ice than viruses with the AD8 Bam Env; after 1 day on ice, viruses with the AD8 Bam Env lost ~45% of their infectivity, whereas the infectivity of the viruses with Tri Bam and AE.1 Bam Envs was unaffected (data not shown). These phenotypes are consistent with State-1 stabilization of the Tri Bam and AE.1 Bam Envs, relative to the AD8 Bam Env (48,113,167).

State-1-destabilizing changes (N197S in gp120, NM 625/626 HT and D674N in gp41) (107) were introduced into the AD8 Bam Env to create the AD8 Bam 197 HT N Env. The AD8 Bam 197 HT N virus was neutralized by the 19b and 17b pNAbs, whereas the AD8 Bam virus was not (Fig. 4A). Both viruses were neutralized comparably by bNAbs. Relative to the AD8 Bam virus, the AD8 Bam 197 HT N virus was inhibited more effectively by BNM-III-170. These phenotypes are consistent with State-1 destabilization of the AD8 Bam 197 HT N Env relative to the AD8 Bam Env.

bioRxiv preprint doi: https://doi.org/10.1101/2022.12.01.518799; this version posted December 2, 2022. The copyright holder for this preprint (which was not certified by peer review) is the author/funder, who has granted bioRxiv a license to display the preprint in perpetuity. It is made available under aCC-BY-NC-ND 4.0 International license.

Compared to the parental AD8 Bam Env, the State-1-stabilized Tri Bam and AE.1 Bam Envs on virus particles were recognized as well by bNAbs and, importantly, only weakly by the V3 and CD4i pNAbs (Fig. 4B). Soluble forms of the gp120 glycoproteins from the AD8 Bam, Tri Bam and AE.1 Bam Envs were precipitated by these pNAbs efficiently (Fig. 4C), indicating that the observed reduction in pNAb binding to the State-1-stabilized Envs on virus particles was not a result of disruption of the epitopes. As a control in this experiment, the recognition of the AE.1 gp120, which contains an R315K change in the V3 region (167), by the 447-52D pNAb was decreased. The R315K change does not affect the binding of the other V3-directed pNAbs (47,170) used in our study.

Interestingly, the antigenicity of the AD8 Bam 197 HT N Env displayed the opposite trends. Compared with the parental AD8 Bam Env, the AD8 Bam 197 HT N Env was recognized less well by bNAbs (PG16, PGT145 and 35O22) with epitopes dependent on quaternary Env structure (Fig. 4B). Conversely, recognition of the AD8 Bam 197 HT N Env by V3 and CD4i pNAbs was relatively increased.

To examine whether the antigenic differences between these State-1-stabilized and -destabilized Envs might be influenced by the oligomeric state of the Env variants, virus particles containing the Env variants were crosslinked with the BS3 crosslinker. The parental AD8 Bam, State-1-destabilized AD8 Bam 197 HT N and State-1-stabilized Tri Bam envelope glycoproteins were crosslinked to trimers with equal efficacy (Fig. 4D).

bioRxiv preprint doi: https://doi.org/10.1101/2022.12.01.518799; this version posted December 2, 2022. The copyright holder for this preprint (which was not certified by peer review) is the author/funder, who has granted bioRxiv a license to display the preprint in perpetuity. It is made available under aCC-BY-NC-ND 4.0 International license.

To summarize, HIV-1 Envs with varying degrees of State-1 stability retain trimeric configurations on virus particles. The spontaneous exposure of V3 and CD4i pNAb epitopes on the cleaved Env trimer is inversely related to the degree of State-1 stability. State-1-stabilized Envs effectively maintain the epitopes recognized by bNAbs, particularly those dependent on quaternary conformation. By contrast, the State-1-destabilized Env was recognized inefficiently by bNAbs.

Shedding of gp120 from virus particles.

The non-covalent association of gp120 with the Env trimer is prone to disruption, either spontaneously or in response to the binding of ligands (sCD4, CD4-mimetic compounds) that induce Env conformations downstream of State 1 (137-139,161,171). We set out to study the shedding of gp120 from Envs with different degrees of State-1 stability on virus particles produced by IMCs. To establish optimal assay conditions, we measured gp120 shedding from the AD8 Bam Env after a one-hour incubation with different concentrations of sCD4 or the CD4mc BNM-III-170 at various temperatures (Fig. 5A). Both sCD4 and BNM-III-170 induced gp120 shedding in a dose-dependent manner. For both sCD4 and BNM-III-170, shedding of gp120 was slightly more efficient at lower temperatures than at 25° or 37°C. At the highest sCD4 and BNM-III-170 concentrations tested, ~6-10% of the total gp120 on the virus particles was shed after a 1-hour incubation at 0° or 4°C.

The resistance of closely matched HIV-1 Env variants to inhibition by CD4mcs is a valuable indicator of the degree of State-1 stabilization (167). To determine whether CD4mc-induced gp120 shedding correlates with this functional phenotype, we

bioRxiv preprint doi: https://doi.org/10.1101/2022.12.01.518799; this version posted December 2, 2022. The copyright holder for this preprint (which was not certified by peer review) is the author/funder, who has granted bioRxiv a license to display the preprint in perpetuity. It is made available under aCC-BY-NC-ND 4.0 International license.

compared BNM-III-170-induced shedding of gp120 from virus particles with the AD8 Bam, AD8 Bam 197 HT N, Tri Bam and AE.1 Bam Envs (Fig. 5B). Both State-1-stabilized Envs, Tri Bam and AE.1 Bam, were less sensitive to gp120 shedding induced by BNM-III-170 than the AD8 Bam Env.

In HIV-1 variants with closely matched Envs, resistance to cold inactivation is another useful indicator of the degree of State-1 stabilization (167,172,173). We sought to evaluate the relationship between Env conformation and the spontaneous shedding of gp120 at different temperatures. In initial experiments, we incubated virus particles with the AD8 Bam Env at different temperatures for various times and measured the amount of shed gp120 (Fig. 5C). Shedding of gp120 was significantly greater after incubation of the viruses on ice than at higher temperatures. Thus, the inactivation of the infectivity of viruses with the AD8 Bam Env by incubation on ice coincides with destabilization of the Env trimer and loss of the gp120 subunit.

To evaluate whether HIV-1 Envs stabilized in a pretriggered (State-1) conformation could better resist cold-induced gp120 shedding, we took two approaches. First, we incubated viruses with the AD8 Bam Env on ice in the absence or presence of BMS-806, which stabilizes the State-1 Env conformation (12,21,38,95,118). Treatment with BMS-806 effectively prevented gp120 shedding from the AD8 Bam Env even after an 8-day incubation on ice (Fig. 5D). Second, we compared gp120 shedding at 0° C for viruses with State-1-stabilizing and -destabilizing changes in Env. The State-1-stabilized Envs, Tri Bam and AE.1 Bam, retained gp120 even after a 6-day incubation on ice,

bioRxiv preprint doi: https://doi.org/10.1101/2022.12.01.518799; this version posted December 2, 2022. The copyright holder for this preprint (which was not certified by peer review) is the author/funder, who has granted bioRxiv a license to display the preprint in perpetuity. It is made available under aCC-BY-NC-ND 4.0 International license.

whereas the parental AD8 Bam and the State-1-destabilized AD8 Bam 197 HT N Envs shed much of their gp120 subunits during this time period (Fig. 5E).

To summarize, incubation at 0°C leads to destabilization of the HIV-1 AD8 Bam Env trimer on virus particles, resulting in gp120 shedding. Envs stabilized in a pretriggered (State-1) conformation are better able to resist the trimer-destabilizing effects of exposure to cold. Measurements of gp120 shedding from virus particles correlate well with virus functional phenotypes and can serve as useful indicators of Env conformational state, even for Envs with limited ability to support HIV-1 infection.

Effects of 0°C incubation on the antigenicity of a State-1-stabilized Env.

Although the State-1-stabilized Tri Bam Env did not shed gp120 after prolonged incubation on ice, other more subtle changes to the conformation of the Tri Bam Env trimer might have resulted from cold exposure. To address this, we compared the antigenicity of the Tri Bam Env after a 7-day incubation on ice with that of a Tri Bam Env not incubated on ice (Fig. 6). Exposure to 0°C for 7 days had little effect on the amount of Tri Bam Env on the virus particles or on its recognition by bNAbs or pNAbs. We note that the V3 and CD4i pNAbs mainly recognize the uncleaved Tri Bam Env on the virus particles, and any low-level recognition of gp120 by these antibodies was not accompanied by coprecipitation of gp41. We conclude that the effects of the Q114E, Q567K and A582T changes on Env conformation allow the virion Env trimers to withstand cold stress for at least one week.

Characterization of virion Envs from other HIV-1 strains.

bioRxiv preprint doi: https://doi.org/10.1101/2022.12.01.518799; this version posted December 2, 2022. The copyright holder for this preprint (which was not certified by peer review) is the author/funder, who has granted bioRxiv a license to display the preprint in perpetuity. It is made available under aCC-BY-NC-ND 4.0 International license.

The studies above utilized closely matched HIV-1_{AD8} Env variants with amino acid residue changes that specifically alter Env triggerability (107,167); analysis of these variants identified useful phenotypic indicators of the degree of State-1 stabilization. To examine whether these conformational indicators could be generalized to Envs from other HIV-1 strains, we studied the laboratory-adapted, tier-1 HIV-1_{NL4-3} (clade B); the primary, tier-2/3 HIV-1_{JR-FL} (clade B); and the primary, tier-2/3 HIV-1_{BG505} (clade A). HIV-1_{JR-FL} and HIV-1_{BG505} Envs are of particular interest because pseudoviruses with these Envs exhibit levels of resistance to cold inactivation and CD4mc inhibition that are comparable to those of pseudoviruses with the AD8 Env containing the State-1-stabilizing changes examined here (167). The JR-FL E168K Env variant was used in the analysis of Env antigenicity as the E168K change in the gp120 V2 region allows recognition by the V2 quaternary bNAbs, PG16 and PGT145, without detectable effects on other properties of the HIV-1_{JR-FL} Env (92,147,148,164). Comparing the antigenicity of the Env variants on virus particles (Fig. 7A), we noted trends similar to those observed for the AD8 Bam Env variants: (i) the cleaved Env in the more triggerable NL4-3 Env was not efficiently precipitated by the bNAbs (PG16, PGT145, PGT151 and 35O22) that recognize epitopes dependent on quaternary Env structure; nonetheless, the NL4-3 virus was efficiently neutralized by the PG16 and PGT145 antibodies (data not shown); (ii) the cleaved JR-FL E168K Env was precipitated by all the bNAbs but, with the exception of weak precipitation by the 19b and 447-52D V3 pNAbs, not by most pNAbs; and (iii) although the level of cleaved BG505 Env on the virus particles was very low, this small amount of cleaved Env was detected better by the bNAbs than by pNAbs. Deglycosylation of the precipitated BG505 Env proteins confirmed the efficient recognition of gp120 by all the bNAbs tested, with detectable recognition of gp120 by

bioRxiv preprint doi: https://doi.org/10.1101/2022.12.01.518799; this version posted December 2, 2022. The copyright holder for this preprint (which was not certified by peer review) is the author/funder, who has granted bioRxiv a license to display the preprint in perpetuity. It is made available under aCC-BY-NC-ND 4.0 International license.

the 19b and 447-52D V3 pNAbs and by the 17b and E51 CD4i pNAbs (data not shown). We confirmed that the pNAb epitopes are present on the gp120 glycoproteins of these three HIV-1 strains (with the exception of the 19b V3 epitope on the NL4-3 Env) (Fig. 7B).

We examined the shedding of gp120 from viral particles containing Envs from the different HIV-1 strains in response to the CD4mc BNM-III-170 and to ice exposure (Fig. 7C). The NL4-3 Env shed gp120 efficiently following incubation with BNM-III-170 or on ice. By contrast, the JR-FL and BG505 Envs shed gp120 minimally in response to the CD4mc or cold exposure. These gp120 shedding efficiencies correlate with the susceptibility of these viruses to cold inactivation or inhibition by BNM-III-170 (167). Thus, the antigenicity and gp120 shedding assays using IMC-generated virus particles revealed important distinctions among Envs with different triggerability levels, even for Envs derived from different HIV-1 strains and clades. Additionally, viruses produced from cells transfected with IMCs may demonstrate improved Env proteolytic processing in cases, e.g., the JR-FL and BG505 Envs, where low levels of Env cleavage have been observed in the transfected cells (Fig. 7D) (167). However, even when produced by an IMC, the BG505 Env still displayed a very low level of cleavage in cell lysates and on virus particles. Therefore, a high level of cleaved Env on virus particles is one criterion that could be used to prioritize HIV-1 strains for structural and immunogenicity studies of membrane Envs.

Characterization of Env in virions produced from infected T cells.

bioRxiv preprint doi: https://doi.org/10.1101/2022.12.01.518799; this version posted December 2, 2022. The copyright holder for this preprint (which was not certified by peer review) is the author/funder, who has granted bioRxiv a license to display the preprint in perpetuity. It is made available under aCC-BY-NC-ND 4.0 International license.

The above analyses were performed with virus particles produced transiently from transfected 293T cells. To examine whether the observed Env phenotypes would also be associated with virions produced from infected T cells, we analyzed the antigenicity of the AD8 Bam Env and the E.1 Bam Env in virions produced from infected C8166-R5 cells. C8166-R5 cells are human $CD4^+$ T lymphocytes transformed by human T-cell leukemia virus (HTLV-I) and transduced with a vector expressing human CCR5 (174). The E.1 Bam Env is identical to the AE.1 Bam Env except that one of the State-1-stabilizing changes, A582T, has been reverted (167). The E.1 Bam Env was studied here instead of the Tri Bam or AE.1 Bam Envs because the E.1 Bam Env was more infectious in C8166-R5 cells, but nonetheless retained most State-1-stabilized phenotypes (reference 167 and data not shown). The AD8 Bam Env on infectious virions produced in C8166-R5 cells displayed an antigenic pattern similar to that of the virus particles produced from transfected 293T cells, i.e., gp120 was recognized by bNAbs and V3 and CD4i pNAbs, but the coprecipitation of gp41 was less efficient for the pNAbs than for the bNAbs (Fig. 8A). Relative to the antigenicity of AD8 Bam Env, the cleaved E.1 Bam Env on virions demonstrated strong bNAb binding and decreased pNAb binding. The consistency between the antigenicity of Envs on viruses produced from transfected 293T cells and an infected T cell line support the generality and intrinsic nature of the observed Env phenotypes.

In multiple repeat experiments, we noted that the binding of the cleaved E.1 Bam Env by V3 and CD4i pNAbs was variable and, in some cases, at a level comparable to that of the AD8 Bam Env (see average values in Fig. 8A, right panel). Because C8166-R5 cells express CD4 that could potentially interact with HIV-1 Env (175,176), we tested

bioRxiv preprint doi: https://doi.org/10.1101/2022.12.01.518799; this version posted December 2, 2022. The copyright holder for this preprint (which was not certified by peer review) is the author/funder, who has granted bioRxiv a license to display the preprint in perpetuity. It is made available under aCC-BY-NC-ND 4.0 International license.

whether CD4 coexpression could affect the conformation of a State-1-stabilized Env on virus particles. To that end, we transfected 293T cells with the E.1 Bam IMC with or without a plasmid expressing human CD4. Analysis of the E.1 Bam Env antigenicity on virus particles showed that coexpression of CD4 resulted in modest increases in the binding of V3 and CD4i pNAbs to gp120, without accompanying increases in the coprecipitation of gp41 (Fig. 8B). We conclude that coexpression of CD4 in cells producing virus particles can in some circumstances lead to an increased sampling of non-State-1 Env conformations on the viral particles.

DISCUSSION

The development of an effective AIDS vaccine has been frustrated by the inefficiency with which current Env immunogens, including stabilized soluble trimers, elicit neutralizing antibodies with breadth against primary HIV-1 strains (64-75). The evolution of bNAbs during natural HIV-1 infection likely is driven by the mature (cleaved) State-1 Env trimer on viral or cell membranes. The association of Env with the membrane is important for maintaining a State-1 Env conformation and for the correct composition of Env glycans (11,90-93,102-113), both of which can potentially influence the binding of bNAbs and their precursors.

Virus-like particles (VLPs) offer a means to access native, functional HIV-1 Envs in a natural membrane context. Indeed, several groups have explored VLP Env composition, antigenicity, structure, dynamics and immunogenicity (12,95,118,121-137,177-179). Structural and conformational heterogeneity in VLP Envs complicates efforts to characterize the virion spike and to develop these membrane Envs as

bioRxiv preprint doi: https://doi.org/10.1101/2022.12.01.518799; this version posted December 2, 2022. The copyright holder for this preprint (which was not certified by peer review) is the author/funder, who has granted bioRxiv a license to display the preprint in perpetuity. It is made available under aCC-BY-NC-ND 4.0 International license.

546 immunogens presenting a pretriggered (State-1) conformation to the immune system.
547 One important source of conformational heterogeneity is the uncleaved gp160 Env,
548 which is flexible and binds multiple pNAbs (40-45). In this study, we utilized infectious
549 molecular clones (IMCs) to produce virus particles with sufficient levels of cleaved HIV-1
550 Env for detailed analysis of Envs on virus particles. In this respect, virus particles
551 produced by IMCs were superior to pseudotyped viruses, where Env cleavage was
552 inefficient and not sufficiently increased by lowering the amount of Env-expressing
553 plasmid transfected with the Gag-expressing plasmid. Our results are consistent with
554 those of previous studies (136,180). In one such study (136), extremely low ratios (e.g.,
555 1:80) of Env:Gag expressor plasmids were required to achieve a level of Env cleavage
556 comparable to that produced by an IMC. At such low Env:Gag ratios, the low levels of
557 Env on the VLPs create additional impediments to the characterization of the virion
558 Envs. In addition to the use of IMCs, we also utilized Western blotting that could
559 distinguish the phenotypes of cleaved and uncleaved Envs; this distinction is essential
560 for characterizing the conformations of the different Env populations present on virus
561 particles.
562
563 In contrast to pseudotyped viruses, IMC-produced virus particles generally
564 exhibited levels of cleaved Env similar to those in virions produced from infected T cells.
565 The infectivity of IMC-produced viruses can be inactivated by the introducing
566 conservative changes that eliminate reverse transcriptase, RNAse H or integrase
567 expression without compromising the enrichment of cleaved Env on the virus particles.
568 Disruption of *vif*, *vpr*, *vpu* and *nef* also did not affect Env amount or level of cleavage on
569 the virus particles (Fig.1D). Combinations of these inactivating mutations could be

bioRxiv preprint doi: https://doi.org/10.1101/2022.12.01.518799; this version posted December 2, 2022. The copyright holder for this preprint (which was not certified by peer review) is the author/funder, who has granted bioRxiv a license to display the preprint in perpetuity. It is made available under aCC-BY-NC-ND 4.0 International license.

introduced into IMCs to minimize the possibility of infectious virus in VLP preparations. Vpu and Nef contribute to the down-regulation of CD4-Env complexes on the surface of infected cells and virions, and therefore could be of value in VLP-producing cells that express CD4 (176,181-185). However, we found that even with intact *vpu* and *nef* genes on the IMC, CD4 expression in the producer cell increased the exposure of CD4-induced pNAb epitopes on the VLP Env (Fig. 8B). Using CD4-negative producer cells avoids this potential problem. The HIV-1 protease, which was left intact on the IMCs to allow proteolytic maturation of the VLPs, can also clip the cytoplasmic tail of Env from some HIV-1 strains (143,144). We found that this cytoplasmic tail clipping was enhanced by chimerism of the HIV-1_{AD8} Env construct near the cleavage site and could be remedied by changes near the junction sequences. Nonetheless, cytoplasmic tail clipping exerted no detectable effect on AD8 Env antigenicity or neutralization sensitivity. These results are consistent with previous studies showing that complete truncation of the HIV-1_{AD8} Env cytoplasmic tail does not detectably affect virus neutralization sensitivity (94).

IMC-produced virus particles with high levels of cleaved Env allowed direct analysis of the virion Env population, essentially all of which is trimeric. The antigenicity and gp120 shedding analyses revealed the existence of at least three populations of cleaved AD8 Env trimers (Fig. 9A):

1) Pretriggered (State-1) Env – This cleaved Env population is marked by its recognition by bNAbs but not pNAbs. This Env population is maintained after treatment with BMS-806 and crosslinkers and is increased by Env changes that stabilize the

bioRxiv preprint doi: https://doi.org/10.1101/2022.12.01.518799; this version posted December 2, 2022. The copyright holder for this preprint (which was not certified by peer review) is the author/funder, who has granted bioRxiv a license to display the preprint in perpetuity. It is made available under aCC-BY-NC-ND 4.0 International license.

pretriggered conformation (167). Notably, as seen in the ability of gp120- or gp41-directed bNAbs to coprecipitate the other subunit, the Env trimers in this population are stable in detergent lysates. This Env population also is more resistant to gp120 shedding induced by incubation on ice or with CD4mc. Lower Env triggerability and increased State-1 occupancy are often associated with increased intersubunit interactions that stabilize the trimer (38,167). In agreement with this, BMS-806-treated and State-1-stabilized Envs are relatively resistant to gp120 shedding after exposure to 0° C or detergent. The cleaved, State-1-stabilized Tri Bam Env on the virus surface maintained its antigenicity for at least one week on ice.

2) Envs in more open conformations – This cleaved Env population is marked by its recognition by V3 and CD4i pNAbs. This Env population is decreased by treatment with BMS-806 or crosslinkers or by the introduction of State-1-stabilizing changes in Env (167). Conversely, this Env population is increased by State-1-destabilizing Env changes that promote CD4 independence (107), by the binding of sCD4 to Env on virus particles, and by CD4 coexpression in virus-producing cells. These cleaved Env trimers apparently represent more open conformations downstream of State 1. The intersubunit interactions in these trimers are more labile than those in the State-1 Envs, as gp120-directed pNAbs less efficiently coprecipitate gp41 in detergent lysates.

3) gp41 molecules not detectably associated with gp120 – This gp41-only population is marked by its recognition by C34-Ig and the F240 pNAb, which detect gp41 molecules after gp120 has been shed (21,158,186). As seen in our results, the gp41 from this population is precipitated by C34-Ig and F240, but gp120 is not coprecipitated. State-1

bioRxiv preprint doi: https://doi.org/10.1101/2022.12.01.518799; this version posted December 2, 2022. The copyright holder for this preprint (which was not certified by peer review) is the author/funder, who has granted bioRxiv a license to display the preprint in perpetuity. It is made available under aCC-BY-NC-ND 4.0 International license.

618 stabilization by Env changes or BMS-806 treatment reduces gp120 shedding and
619 decreases the level of gp41-only Envs, implying that the gp41-only population increases
620 under conditions in which more open Env conformations are favored.
621
622 Our results support a model in which the triggerability or reactivity of Env variants
623 determines the spontaneous occupancy of the three cleaved Env populations on the
624 virus particles (12,48,49,107,113,167-169) (Fig. 9B). Virions with the tier-2 AD8 Bam
625 Env, with an intermediate level of triggerability (167), contain all three cleaved Env
626 populations in the following order of decreasing amount: pretriggered ≥ open >>> gp41-
627 only. Virions with the more triggerable tier-1 NL4-3 Env and the CD4-independent AD8
628 Bam 197 HT N Env contain all three populations in the following order of decreasing
629 amount: open > pretriggered >>> gp41-only. Virions with the State-1-stabilized Tri Bam
630 and AE.1 Bam Envs and virions with the tier-2/3 JR-FL and BG505 Envs contain only
631 two populations in the following order of decreasing amount: pretriggered > open. We
632 suggest that the lower triggerability or reactivity of this last group of Env variants is
633 related to the higher activation energy barrier separating the pretriggered (State-1)
634 conformation and downstream, more open conformations, leading to higher occupancy
635 of the pretriggered state on the virus particles (107,168).
636
637 The degree to which the cleaved Env trimers on virus particles sample State 1 or
638 more open conformations is subject to modulation (Fig. 9C). CD4 binding promotes
639 HIV-1 entry by stimulating Env transitions from State 1 to downstream conformations
640 (12). Spontaneous transitions from the pretriggered (State-1) conformation of Env can
641 be inhibited by treatment of the virions with BMS-806 (21), by crosslinking, or by the

bioRxiv preprint doi: https://doi.org/10.1101/2022.12.01.518799; this version posted December 2, 2022. The copyright holder for this preprint (which was not certified by peer review) is the author/funder, who has granted bioRxiv a license to display the preprint in perpetuity. It is made available under aCC-BY-NC-ND 4.0 International license.

introduction of State-1-stabilizing changes in Env. Conversely, treatment of the virions with sCD4 or a CD4mc, or the introduction of State-1-destabilizing changes in Env can promote Env transitions from State 1 to more open downstream conformations. These downstream Env conformations are recognized by pNAbs that bind the coreceptor-interactive region of gp120, consistent with their potential relevance to virus entry events following CD4 engagement. We note that crosslinking reduces the binding of these pNAbs to the unliganded AD8 Env (Fig. 2D), suggesting that Env flexibility contributes to the spontaneous exposure of the pNAb epitopes. This is consistent with smFRET observations indicating that State-1 Envs spontaneously and reversibly sample conformations that resemble the States 2 and 3 induced by CD4 (12). If these epitopes are accessible on the unliganded virion Env, why don't the V3 and CD4i pNAbs neutralize HIV-1_{AD8}? The lability of gp120-trimer association observed for the AD8 Env population that spontaneously exposes pNAb epitopes hints that these Envs may be inherently dysfunctional or that their functionality is short-lived. Poorly functional Envs with exposed pNAb epitopes have been previously observed on VLPs and were shown to be more susceptible to digestion with a cocktail of proteases (127). Like the short-lived Env intermediates induced by sCD4 or CD4mcs (187,188), spontaneously sampled, open Env conformations may be labile. To maintain some infectivity, highly triggerable Envs like AD8 Bam 197 HT N may need to acquire adaptive changes to minimize the lability of downstream Env intermediates during virus infection (107). Of note, the complexes formed by virion Env with CD4 on the target cell membrane were found to be significantly more stable than those formed by sCD4 (187).

bioRxiv preprint doi: https://doi.org/10.1101/2022.12.01.518799; this version posted December 2, 2022. The copyright holder for this preprint (which was not certified by peer review) is the author/funder, who has granted bioRxiv a license to display the preprint in perpetuity. It is made available under aCC-BY-NC-ND 4.0 International license.

Our study provides guidance for efforts to improve VLPs as immunogens that present the membrane-anchored, pretriggered (State-1) conformation of HIV-1 Env to the immune system. The first requirement is that VLPs should contain as little gp160 as possible. Uncleaved Env on VLPs or VLP-producing cells is conformationally flexible and could divert desirable immune responses by presenting immunodominant pNAb epitopes to the immune system. Although cleaved Env is generally enriched in virions, some uncleaved Env is found in most VLP preparations. Previous studies with A549 cells stably producing Gag-mCherry VLPs indicated that essentially all of the uncleaved VLP Env passed through the Golgi apparatus (7); the uncleaved Env on VLPs produced in that system was modified by complex carbohydrates resembling those on mature Env. In VLPs produced transiently from 293T cells in this study, some of the uncleaved Env lacks complex glycans, indicating that it may have bypassed the Golgi apparatus. One likely source of this uncleaved Env may be cellular vesicles that contaminate the VLP preparation. The level of vesicle contaminants could be influenced by the choice of producer cells, transient versus stable transfection and the VLP production system. If complete elimination of the uncleaved gp160 Env in VLP preparations is not possible, BMS-806 and long-acting BMS-806 analogues could be used to reduce the exposure of pNAb epitopes on the residual gp160 (38,118).

The second requirement is that cleaved Env should be in a State-1 conformation with minimal spontaneous exposure of pNAb epitopes. We found that even cleaved HIV-1 Env trimers of the tier-2 AD8 Env spontaneously exposed V3 and CD4i pNAb epitopes related to the coreceptor-binding region of gp120. The extent of this exposure appears to be related to Env triggerability, i.e., the propensity of Env to make transitions

bioRxiv preprint doi: https://doi.org/10.1101/2022.12.01.518799; this version posted December 2, 2022. The copyright holder for this preprint (which was not certified by peer review) is the author/funder, who has granted bioRxiv a license to display the preprint in perpetuity. It is made available under aCC-BY-NC-ND 4.0 International license.

689 from the pretriggered (State-1) conformation to downstream conformations (107,168).
690 State-1-stabilizing Env changes, BMS-806 treatment and crosslinking (or combinations
691 of these measures) can decrease the amount of the more open cleaved Envs trimers on
692 the VLPs, even beyond that found in natural HIV-1 strains. As State-1 stabilization
693 improves, Env typically demonstrates decreased ability to mediate virus infection, as
694 expected for lower triggerability (107,167). Assays dependent on functional virus (e.g.,
695 antibody neutralization, cold sensitivity, inhibition by sCD4 or small-molecule entry
696 blockers) cannot be used to study such highly State-1-stabilized Envs. The VLP
697 antigenicity and gp120 shedding assays developed here do not require the virus to be
698 functional, and thus can be applied in broad context to monitor progressive
699 improvements in the stabilization of the pretriggered conformation of Envs from multiple
700 HIV-1 strains. Fortunately, bNAbs and pNAbs broadly reactive with the Envs from
701 diverse HIV-1 are available for the antigenicity analyses, and thus the antigenicity of
702 different HIV-1 strains can be directly compared to allow Env conformations to be
703 deduced.
704
705 The third requirement is that shedding of gp120 from the cleaved Env on VLPs
706 should be minimized. Viruses with the AD8 Bam Env spontaneously shed gp120 after
707 incubation at various temperatures (Fig. 5). Trimer stability after incubation of the VLPs
708 on ice is a better indicator of State-1 stabilization than at higher temperatures
709 (167,172,173). The detrimental effects of ice formation at near-freezing temperatures
710 apparently stress the non-covalent intersubunit interactions on which Env trimer integrity
711 depends (189-191). Further studies of the longevity of State-1-stabilized Env trimers at
712 37°C would be relevant to their inclusion in VLP immunogens, particularly in the

bioRxiv preprint doi: https://doi.org/10.1101/2022.12.01.518799; this version posted December 2, 2022. The copyright holder for this preprint (which was not certified by peer review) is the author/funder, who has granted bioRxiv a license to display the preprint in perpetuity. It is made available under aCC-BY-NC-ND 4.0 International license.

713 presence of adjuvants. Encouragingly, State-1-stabilized Envs like the Tri Bam and
714 AE.1 Bam Envs and the natural JR-FL Env were remarkably resistant to gp120
715 shedding. Using these Envs in VLPs provides alternatives to the use of artificial inter-
716 subunit disulfide bonds like SOS (192-194), which has been reported to destabilize
717 State 1 in virion Envs (95, 118).
718
719 The fourth requirement is that VLP-producing cells should not coexpress CD4.
720 CD4 expression in the VLP-producing cells was found to exert subtle effects on the
721 exposure of pNAb epitopes on the VLP Envs, even for Vpu^+ Nef^+ proviruses (Fig. 8B).
722 The use of CD4-negative cells to produce VLPs enriched in State-1 Envs seems
723 advisable.
724
725 Advances in understanding the pretriggered (State-1) conformation of HIV-1
726 Envs and learning how to preserve this labile state, together with the assays established
727 here, should assist efforts to elicit effective antibody responses with VLP and other
728 immunogen formulations.
729

bioRxiv preprint doi: https://doi.org/10.1101/2022.12.01.518799; this version posted December 2, 2022. The copyright holder for this preprint (which was not certified by peer review) is the author/funder, who has granted bioRxiv a license to display the preprint in perpetuity. It is made available under aCC-BY-NC-ND 4.0 International license.

MATERIALS AND METHODS

Plasmids. The HIV-1_{AD8}, HIV-$1_{AE.2}$ and HIV-1_{JR-FL} *env* sequences for the construction of IMCs were obtained from the respective pSVIIIenv expression vectors (167). Relative to the AD8 Env, the AE.2 Env contains the following changes: Q114E, R166K, R178K, R252K, R315K, R419K, R557K, Q567K, A582T, R633K, Q658K, A667K and N677K. The Kpn I – BamHI *env* fragments from pSVIIIenv AD8 and pSVIIIenv AE.2 were introduced into the pNL4-3 IMC, using an intermediary vector, pE7SB-NL4-3. The pE7SB-NL4-3 plasmid contains the Sal I – BamHI fragment of the HIV-1_{NL4-3} provirus, which includes the *tat*, *rev*, *vpu* and 5' *env* genes. The Kpn I – BamHI *env* fragments from the pSVIIIenv plasmids were cloned into the corresponding sites of pE7SB-NL4-3 using Long Ligase (Takara) following the manufacturer's protocol. The Sal I – BamHI fragments from the pE7SB-NL4-3 intermediate plasmids were cloned into the corresponding sites of pNL4-3, which contains the infectious HIV-1_{NL4-3} provirus (NIH HIV Reagent Program). The resulting pNL4-3.AD8 and pNL4-3.AE.2 IMCs express AD8 and AE.2 Envs with N-terminal residues 1-33 (including the signal peptide) and C-terminal residues 751-856 (C-terminus of Env cytoplasmic tail) from the NL4-3 Env.

The pNL4-3.AD8 Bam and pNL4-3.AE.2 Bam IMC was created by introducing mutations encoding S752F and I756F changes in the Env cytoplasmic tail into pNL4-3.AD8 and pNL4-3.AE.2 using primers forward: tccgtgcgattagtggatggatTcttggcacttTtctgggacgatctgcggagcctgtgcctcttca, reverse: tctgtctctgtctctgtctccaccttcttcttcgattccttcgggcctgtcgggtcccctcggggct. The pNL4-3.AD8(-) IMC encodes an AD8 Env in which the REKR cleavage site (residues 508-511) is

bioRxiv preprint doi: https://doi.org/10.1101/2022.12.01.518799; this version posted December 2, 2022. The copyright holder for this preprint (which was not certified by peer review) is the author/funder, who has granted bioRxiv a license to display the preprint in perpetuity. It is made available under aCC-BY-NC-ND 4.0 International license.

753 altered to SEKS. The pNL4-3.AD8 Δ712 plasmid encodes an AD8 Env with a truncated
754 cytoplasmic tail (missing residues 712-856).
755
756 To knock out HIV-1 genes in the pNL4-3.AD8 plasmid, stop codons were
757 introduced individually into the open reading frames encoding RT, RNAse H, IN, Vif,
758 Vpr, Vpu and Nef. The primers for these knockouts were: RT forward:
759 TTTAAATTTTtaaATTAGTCCTATTGAGACTGTAC, reverse:
760 GTGCAGCCAATCTGAGTC; RNAse H forward: AAACTTTCTAaGTAGATGGGGC,
761 reverse: CTGCTCCTATTATGGGTTC; IN forward:
762 AAAGTACTATaaTTAGATGGAATAGATAAGGC, reverse: CCTGATTCCAGCACTGAC;
763 Vif forward tgaggattaacacaTAGaaaagattagtaaaa, reverse
764 tcctgtctacttgccacacaatcatcacctgc; Vpr forward:
765 actgacagaggacagatggaaTAAgccccagaagaccaa, reverse:
766 ttcctaacactaggcaaaggtggctttatctgtt; Vpu forward:
767 TAgcaacctataatagtagcaatagtagcattagtagtagca reverse:
768 tacatgtactacttactgctttgatagagaagcttgat Nef forward: TAAggtggcaagtggtcaaaaagtagtgtga
769 reverse: cttatagcaaaatcctttccaagccctgtctt .
770
771 IMCs encoding the Tri Bam and AD8 Bam 197 HT N Envs were made by
772 introducing Q114E + Q567K + A682T or N197S + NM 625/626 HT + D674N changes,
773 respectively, into pNL4-3.AD8 Bam IMC.
774
775 The pNL4-3.AE.1 Bam IMC was cloned from pNL4-3.AE.2 Bam by back reverting
776 the following lysine residues: K658Q, K667A and K677N. The pNL4-3.E.1 Bam was

bioRxiv preprint doi: https://doi.org/10.1101/2022.12.01.518799; this version posted December 2, 2022. The copyright holder for this preprint (which was not certified by peer review) is the author/funder, who has granted bioRxiv a license to display the preprint in perpetuity. It is made available under aCC-BY-NC-ND 4.0 International license.

777 cloned by back reverting T582A in pNL4-3.AE.1 Bam. The Strep tag was inserted at the
778 C terminus by site-directed mutagenesis using primers forward:
779 CCCAGTTCGAGAAAtaagatgggtggcaagtggtcaaaaagtagtgtgat, reverse:
780 GGTGGCTCCAtagcaaaatcctttccaagccctgtcttattcttctaggta.
781
782 To create IMCs expressing soluble gp120s, the codon for gp120 residue 508 was
783 replaced by a stop codon. All site-directed mutagenesis with IMCs was done using the
784 Q5 high-fidelity DNA polymerase (New England Biolabs) and One Shot Stbl3
785 Chemically Competent E. coli (Invitrogen) following the manufacturer's protocols.
786
787 To clone the pNL4-3.JR-FL IMC, an overlap extension PCR using PfuUltra II
788 fusion HS DNA Polymerase (Agilent) was performed. The primers and template
789 plasmids are as follows: AD8 Sal I forward (CAACAACTGCTGTTTATCC) and
790 AD8/JRFL Env reverse (ctgtagcactacagatcatc) using the pNL4-3.AD8 template;
791 AD8/JRFL Env forward (gatgatctgtagtgctacag) and JRFL BamHI reverse
792 (gtcccagataagtgccaag) using the pSVIIIenv JR-FL template (167). The resulting Sal I –
793 BamHI *vpu*$_{NL4-3}$-*env*$_{JR-FL}$ fragment was transferred to the pNL4-3.AD8 vector using Long
794 Ligase.
795
796 To clone the pNL4-3.BG505 IMC, an overlap extension PCR was performed.
797 The primers and template plasmids are as follows: pNL4-3.AD8 Sal I forward
798 (CAACAACTGCTGTTTATCCATTTCAGAATTG) and BG505 vpu reverse
799 (AATTTCCAAAGGAAGCATtacatgtactacttactg) using the pNL4-3.AD8 template; BG505
800 vpu forward (cagtaagtagtacatgtaATGCTTCCTTTGGAAATT) and pcDNA BG505 BamHI

bioRxiv preprint doi: https://doi.org/10.1101/2022.12.01.518799; this version posted December 2, 2022. The copyright holder for this preprint (which was not certified by peer review) is the author/funder, who has granted bioRxiv a license to display the preprint in perpetuity. It is made available under aCC-BY-NC-ND 4.0 International license.

mut reverse (GCAAGAGCTAAGgATCCGCTCAC) using the pcDNA3.1 BG505 template (NIH HIV Reagent Program). The Sal I – BamHI *vpu*$_{BG505}$-*env*$_{BG505}$ fragment was transferred to the pNL4-3.AD8 vector using Long Ligase.

Antibodies and sCD4. The following reagents were obtained through the NIH HIV Reagent Program, Division of AIDS, NIAID, NIH: VRC03, PGT121, 4E10, 10E8.v4, 39F, 3074, 3869, 17b, E51 and sCD4.

Cell lines. HEK 293T, HeLa cells and TZM-bl cells (ATCC) were cultured in Dulbecco's modified Eagle's medium (DMEM) supplemented with 10% fetal bovine serum (FBS) and 100 µg/ml penicillin-streptomycin (Life Technologies). CCR5-expressing C8166-R5 T cells were cultured in Roswell Park Memorial Institute (RPMI) 1640 medium supplemented with 10% FBS and 100 µg/ml penicillin-streptomycin; 1 µg/ml of puromycin was added every fifth passage.

Env expression and incorporation into virus particles. To prepare pseudoviruses, 293T cells were cotransfected using polyethyleneimine (PEI, Polysciences) with an Env-expressor plasmid, a Tat-encoding plasmid and the pNL4-3.ΔEnv plasmid (renamed from pNL4-3.Luc.R-E- plasmid, available at the NIH HIV Reagent Program) at a 1:0.125:1 weight ratio unless indicated otherwise. To prepare replication-competent viruses, 293T cells were transfected with the pNL4-3.Env plasmid using PEI. The medium was replaced at 4-6 h after transfection. Lipofectamine 3000 (Invitrogen) was used to transfect HeLa cells following the manufacturer's protocol. At 48 h to 72 h after transfection, cells were lysed and clarified; supernatants were collected, filtered (0.45

bioRxiv preprint doi: https://doi.org/10.1101/2022.12.01.518799; this version posted December 2, 2022. The copyright holder for this preprint (which was not certified by peer review) is the author/funder, who has granted bioRxiv a license to display the preprint in perpetuity. It is made available under aCC-BY-NC-ND 4.0 International license.

μm) and pelleted at 14,000-100,000 x g for 1 h at 4°C. Virus pellets and clarified cell lysates were then analyzed by Western blotting using a nitrocellulose membrane and wet transfer (350 A, 75 min, Bio-Rad). Western blots were developed with 1:2,000 goat anti-gp120 polyclonal antibody (Invitrogen), 1:2,000 4E10 anti-gp41 antibody, 1:1,000 mouse anti-p24 serum (John C. Kappes, University of Alabama at Birmingham), 1:10,000 rabbit anti-hsp70 (K-20) antibody (Santa Cruz Biotechnology). The HRP-conjugated secondary antibodies were 1:2,000 rabbit anti-goat (Invitrogen), 1:2,000 goat anti-human (Invitrogen), 1:1,000 goat anti-mouse (Invitrogen) and 1:10,000 goat anti-rabbit (Sigma-Aldrich). The intensity of protein bands on non-saturated Western blots was quantified using the Bio-Rad Image Lab program. Statistical significance was evaluated by a two-tailed Student's t test.

Virus infectivity. The cell supernatant containing virus was clarified by low-speed centrifugation (2,000 rpm for 10 min). To compare the infectivity of different viruses, an equal volume of clarified supernatant was incubated with TZM-bl cells in 96-well plates (2×10^4 cells per well). The plates were incubated at 37°C/5% CO_2 for 48 h, after which the cells were lysed and luciferase activity was measured using a luminometer.

Virus neutralization. Approximately 100 to 200 $TCID_{50}$ (50% tissue culture infectious dose) of virus was incubated with serial dilutions of purified antibodies, sCD4-Ig or BNM-III-170 at 37°C for 1 h. The mixture was then added to TZM-bl cells in 96-well plates and luciferase activity was measured after 48 h as described above. The concentrations of antibodies and other inhibitors that inhibit 50% of infection (the IC_{50}

bioRxiv preprint doi: https://doi.org/10.1101/2022.12.01.518799; this version posted December 2, 2022. The copyright holder for this preprint (which was not certified by peer review) is the author/funder, who has granted bioRxiv a license to display the preprint in perpetuity. It is made available under aCC-BY-NC-ND 4.0 International license.

values) were determined using GraphPad Prism 8 (five-parameter dose-response) or Microsoft Excel graphs.

Deglycosylation of Env on virus particles. Purified virus particles were first lysed in 1X PBS/0.5% NP-40. The virus lysate was then denatured by boiling in denaturing buffer (New England BioLabs) for 10 min and treated with PNGase F or Endo Hf enzymes (New England BioLabs) for 1.5 h at 37°C in accordance with the manufacturer's protocol. The treated proteins were then analyzed by reducing SDS-PAGE and Western blotting.

Antigenicity of Env on virus particles. To assess Env antigenicity, 50-100-µl aliquots of virus particles (purified and resuspended in 1X PBS) were incubated with a panel of antibodies at 10 µg/mL concentration for 1 h at room temperature. One mL of chilled 1X PBS was added and samples were centrifuged at 14,000 x g for 1 h at 4°C. The pellets were lysed in 100 µl chilled 1X PBS/0.5% NP-40/protease inhibitors cocktail. VLP lysates were rotated during incubation with Protein A-agarose beads for 1 h at 4°C and washed with chilled 1X PBS/0.1% NP-40 three times. The beads were resuspended in 1X PBS containing NuPage LDS Sample Buffer (New England Biolabs) and dithiothreitol (DTT) and used for Western blotting. To prepare the Input (50%) sample, half of the virus volume was mixed with 1 mL chilled 1X PBS and centrifuged at 14,000 x g for 1 h at 4°C; the pellet was resuspended in 1X PBS/LDS/DTT. To examine the effects of soluble CD4 or BMS-806 on Env conformation, 10 µg/mL four-domain sCD4 or 10 µM BMS-806 was first added to virus particles before antibodies were added. To examine the antigenicity of crosslinked Env, a concentrated volume of virus particles

bioRxiv preprint doi: https://doi.org/10.1101/2022.12.01.518799; this version posted December 2, 2022. The copyright holder for this preprint (which was not certified by peer review) is the author/funder, who has granted bioRxiv a license to display the preprint in perpetuity. It is made available under aCC-BY-NC-ND 4.0 International license.

was first incubated with 0.1 mM or 1 mM DTSSP crosslinker for 30 min at room temperature, after which the reaction was quenched with 100 mM Tris-HCl, pH 8.0, for 10 min at room temperature. More PBS was added and Env antigenicity was evaluated as described above.

Oligomerization of Env on virus particles. Purified virus particles were incubated with different concentrations of BS3 crosslinkers (ThermoFisher Scientific) for 30 min at room temperature, after which the reaction was quenched with 100 mM Tris-HCl, pH 8.0, for 10 min at room temperature. LDS/DTT was added and samples were boiled and then analyzed by reducing SDS-PAGE and Western blotting.

Antigenicity of soluble gp120. 293T cells were transfected with IMCs expressing the soluble gp120 version of the AD8 Bam, Tri Bam, AE.1 Bam, NL4-3, JR-FL or BG505 Envs using PEI. Forty-eight hours after transfection, cell supernatants containing the soluble glycoproteins were collected and filtered (0.45 mm). Aliquots were incubated with 10 µg/mL antibody and Protein A-agarose beads, and the mixture was rotated at room temperature for 2 h. The beads were washed three times with 1X PBS/0.1% NP-40 before the beads were boiled and Western blotted with a goat anti-gp120 antibody, as described above. To crosslink soluble gp120, the filtered supernatants from transfected 293T cells were incubated with 1 mM DTSSP for 30 min at room temperature. The reactions were quenched with 100 mM Tris-HCl, pH 8.0, for 10 min before the antigenicity assay was carried out as described above.

bioRxiv preprint doi: https://doi.org/10.1101/2022.12.01.518799; this version posted December 2, 2022. The copyright holder for this preprint (which was not certified by peer review) is the author/funder, who has granted bioRxiv a license to display the preprint in perpetuity. It is made available under aCC-BY-NC-ND 4.0 International license.

Shedding of virus particles. Purified virus particles were resuspended in 1X PBS, aliquoted into 50 μL and incubated with serial dilutions of sCD4 or the CD4mc BNM-III-170 for 1 h at room temperature or the indicated temperatures. Next, 200 μL 1X PBS was added and samples were centrifuged at 14,000 x g for 1 h at 4°C. Then 220 μL of the supernatants was collected and rotated during incubation with Galanthus Nivalis Lectin (GNL)-agarose beads (Vector Laboratories) for 2 h at room temperature. Beads were washed three times with 1X PBS/0.1% NP-40 and processed for Western blotting with a goat anti-gp120 antibody, as described above. To evaluate spontaneous gp120 shedding at different temperatures, aliquots of purified virus particles were incubated on ice or at different temperatures for the indicated amount of time before the samples were processed as described above. An aliquot of the purified virus particles prior to incubation with ligands or at different temperatures was used as the “Input” sample.

Antigenicity of Env virions from infected T cells. 293T cells were transfected with IMCs expressing the Strep-tagged AD8 Bam or E.1 Bam Env using PEI. Seventy-two hours after transfection, the cell supernatants were clarified by low-speed centrifugation and serial dilutions of the virus were used to infect TZM-bl cells. Forty-eight hours later, the luciferase activity in the TZM-bl lysates was measured. Virus $TCID_{50}$ values were calculated using the Reed-Muench method (196,197). Approximately 10^7 C8166-R5 cells at a density of 1 x 10^6 cells/mL were infected with virus at a multiplicity of infection of 0.1 for 5 h or overnight, in the presence of 8 μg/mL polybrene. The cells were then washed and fresh medium was added to dilute the cells to a density of 2.5 x 10^5 cells/mL. At three days after infection, one-quarter of the cells/medium was saved and

bioRxiv preprint doi: https://doi.org/10.1101/2022.12.01.518799; this version posted December 2, 2022. The copyright holder for this preprint (which was not certified by peer review) is the author/funder, who has granted bioRxiv a license to display the preprint in perpetuity. It is made available under aCC-BY-NC-ND 4.0 International license.

diluted 1:4 with fresh medium. Six to seven days after infection, virus particles were collected, purified and concentrated, and Env antigenicity was analyzed as described.

ACKNOWLEDGMENTS

We thank Ms. Elizabeth Carpelan for manuscript preparation. Antibodies against HIV-1 were kindly supplied by John C. Kappes (University of Alabama at Birmingham), Dennis Burton (Scripps), Peter Kwong and John Mascola (Vaccine Research Center NIH), Barton Haynes (Duke University), Hermann Katinger (Polymun), James Robinson (Tulane University), and Marshall Posner (Mount Sinai Medical Center). We thank the NIH HIV Reagent Program for providing additional reagents.

This work was supported by grants from the National Institutes of Health (grant nos. AI 145547, AI 124982, AI 150471, AI 129017 and AI 164562), a grant from Gilead Sciences, and by a gift from the late William F. McCarty-Cooper.

We declare no conflicts of interest.

bioRxiv preprint doi: https://doi.org/10.1101/2022.12.01.518799; this version posted December 2, 2022. The copyright holder for this preprint (which was not certified by peer review) is the author/funder, who has granted bioRxiv a license to display the preprint in perpetuity. It is made available under aCC-BY-NC-ND 4.0 International license.

REFERENCES

1. Wyatt R, Sodroski J. 1998. The HIV-1 envelope glycoproteins: fusogens, antigens, and immunogens. Science 280:1884-8.

2. Chen B. 2019. Molecular mechanism of HIV-1 entry. Trends Microbiol 27:878-891.

3. Willey RL, Bonifacino JS, Potts BJ, Martin MA, Klausner RD. 1988. Biosynthesis, cleavage, and degradation of the human immunodeficiency virus 1 envelope glycoprotein gp160. Proc Natl Acad Sci U S A 85:9580-4.

4. Earl PL, Moss B, Doms RW. 1991. Folding, interaction with GRP78-BiP, assembly, and transport of the human immunodeficiency virus type 1 envelope protein. J Virol 65:2047-55.

5. Pal R, Hoke GM, Sarngadharan MG. 1989. Role of oligosaccharides in the processing and maturation of envelope glycoproteins of human immunodeficiency virus type 1. Proc Natl Acad Sci U S A 86:3384-8.

6. Dewar RL, Vasudevachari MB, Natarajan V, Salzman NP. 1989. Biosynthesis and processing of human immunodeficiency virus type 1 envelope glycoproteins: effects of monensin on glycosylation and transport. J Virol 63:2452-6.

7. Zhang S, Nguyen HT, Ding H, Wang J, Zou S, Liu L, Guha D, Gabuzda D, Ho DD, Kappes JC, Sodroski J. 2021. Dual pathways of human immunodeficiency virus type 1 envelope glycoprotein trafficking modulate the selective exclusion of uncleaved oligomers from virions. J Virol 95:e01369-20.

8. Stein BS, Engleman EG. 1990. Intracellular processing of the gp160 HIV-1 envelope precursor. Endoproteolytic cleavage occurs in a cis or medial compartment of the Golgi complex. J Biol Chem 265:2640-9.

9. Merkle RK, Helland DE, Welles JL, Shilatifard A, Haseltine WA, Cummings RD. 1991. gp160 of HIV-I synthesized by persistently infected Molt-3 cells is terminally glycosylated: evidence that cleavage of gp160 occurs subsequent to oligosaccharide processing. Arch Biochem Biophys 290:248-57.

10. Doores KJ, Bonomelli C, Harvey DJ, Vasiljevic S, Dwek RA, Burton DR, Crispin M, Scanlan CN. 2010. Envelope glycans of immunodeficiency virions are almost entirely oligomannose antigens. Proc Natl Acad Sci U S A 107:13800-5.

11. Go EP, Ding H, Zhang S, Ringe RP, Nicely N, Hua D, Steinbock RT, Golabek M, Alin J, Alam SM, Cupo A, Haynes BF, Kappes JC, Moore JP, Sodroski JG, Desaire H. 2017. A glycosylation benchmark profile for HIV-1 envelope glycoprotein production based on eleven Env trimers. J Virol 91:e02428-16.

bioRxiv preprint doi: https://doi.org/10.1101/2022.12.01.518799; this version posted December 2, 2022. The copyright holder for this preprint (which was not certified by peer review) is the author/funder, who has granted bioRxiv a license to display the preprint in perpetuity. It is made available under aCC-BY-NC-ND 4.0 International license.

12. Munro JB, Gorman J, Ma X, Zhou Z, Arthos J, Burton DR, Koff WC, Courter JR, Smith AB, 3rd, Kwong PD, Blanchard SC, Mothes W. 2014. Conformational dynamics of single HIV-1 envelope trimers on the surface of native virions. Science 346:759-63.

13. Wu L, Gerard NP, Wyatt R, Choe H, Parolin C, Ruffing N, Borsetti A, Cardoso AA, Desjardin E, Newman W, Gerard C, Sodroski J. 1996. CD4-induced interaction of primary HIV-1 gp120 glycoproteins with the chemokine receptor CCR-5. Nature 384:179-83.

14. Trkola A, Dragic T, Arthos J, Binley JM, Olson WC, Allaway GP, Cheng-Mayer C, Robinson J, Maddon PJ, Moore JP. 1996. CD4-dependent, antibody-sensitive interactions between HIV-1 and its co-receptor CCR-5. Nature 384:184-7.

15. Kuhmann SE, Platt EJ, Kozak SL, Kabat D. 2000. Cooperation of multiple CCR5 coreceptors is required for infections by human immunodeficiency virus type 1. J Virol 74:7005-15.

16. Khasnis MD, Halkidis K, Bhardwaj A, Root MJ. 2016. Receptor activation of HIV-1 Env leads to asymmetric exposure of the gp41 trimer. PLoS Pathog 12:e1006098.

17. Ma X, Lu M, Gorman J, Terry DS, Hong X, Zhou Z, Zhao H, Altman RB, Arthos J, Blanchard SC, Kwong PD, Munro JB, Mothes W. 2018. HIV-1 Env trimer opens through an asymmetric intermediate in which individual protomers adopt distinct conformations. Elife 7:e34271.

18. Furuta RA, Wild CT, Weng Y, Weiss CD. 1998. Capture of an early fusion-active conformation of HIV-1 gp41. Nat Struct Biol 5:276-9.

19. Koshiba T, Chan DC. 2003. The prefusogenic intermediate of HIV-1 gp41 contains exposed C-peptide regions. J Biol Chem 278:7573-9.

20. He Y, Vassell R, Zaitseva M, Nguyen N, Yang Z, Weng Y, Weiss CD. 2003. Peptides trap the human immunodeficiency virus type 1 envelope glycoprotein fusion intermediate at two sites. J Virol 77:1666-71.

21. Si Z, Madani N, Cox JM, Chruma JJ, Klein JC, Schon A, Phan N, Wang L, Biorn AC, Cocklin S, Chaiken I, Freire E, Smith AB, 3rd, Sodroski JG. 2004. Small-molecule inhibitors of HIV-1 entry block receptor-induced conformational changes in the viral envelope glycoproteins. Proc Natl Acad Sci U S A 101:5036-41.

22. Chan DC, Fass D, Berger JM, Kim PS. 1997. Core structure of gp41 from the HIV envelope glycoprotein. Cell 89:263-73.

bioRxiv preprint doi: https://doi.org/10.1101/2022.12.01.518799; this version posted December 2, 2022. The copyright holder for this preprint (which was not certified by peer review) is the author/funder, who has granted bioRxiv a license to display the preprint in perpetuity. It is made available under aCC-BY-NC-ND 4.0 International license.

23. Weissenhorn W, Dessen A, Harrison SC, Skehel JJ, Wiley DC. 1997. Atomic structure of the ectodomain from HIV-1 gp41. Nature 387:426-30.

24. Lu M, Blacklow SC, Kim PS. 1995. A trimeric structural domain of the HIV-1 transmembrane glycoprotein. Nat Struct Biol 2:1075-82.

25. Melikyan GB, Markosyan RM, Hemmati H, Delmedico MK, Lambert DM, Cohen FS. 2000. Evidence that the transition of HIV-1 gp41 into a six-helix bundle, not the bundle configuration, induces membrane fusion. J Cell Biol 151:413-23.

26. Wilen CB, Tilton JC, Doms RW. 2012. Molecular mechanisms of HIV entry. Adv Exp Med Biol 726:223-42.

27. Bonsignori M, Liao HX, Gao F, Williams WB, Alam SM, Montefiori DC, Haynes BF. 2017. Antibody-virus co-evolution in HIV infection: paths for HIV vaccine development. Immunol Rev 275:145-160.

28. Kwong PD, Mascola JR. 2018. HIV-1 vaccines based on antibody identification, B cell ontogeny, and epitope structure. Immunity 48:855-871.

29. Sok D, Burton DR. 2018. Recent progress in broadly neutralizing antibodies to HIV. Nat Immunol 19:1179-1188.

30. Stewart-Jones GB, Soto C, Lemmin T, Chuang GY, Druz A, Kong R, Thomas PV, Wagh K, Zhou T, Behrens AJ, Bylund T, Choi CW, Davison JR, Georgiev IS, Joyce MG, Kwon YD, Pancera M, Taft J, Yang Y, Zhang B, Shivatare SS, Shivatare VS, Lee CC, Wu CY, Bewley CA, Burton DR, Koff WC, Connors M, Crispin M, Baxa U, Korber BT, Wong CH, Mascola JR, Kwong PD. 2016. Trimeric HIV-1-Env structures define glycan shields from Clades A, B, and G. Cell 165:813-26.

31. Lee JH, Ozorowski G, Ward AB. 2016. Cryo-EM structure of a native, fully glycosylated, cleaved HIV-1 envelope trimer. Science 351:1043-8.

32. Ward AB, Wilson IA. 2017. The HIV-1 envelope glycoprotein structure: nailing down a moving target. Immunol Rev 275:21-32.

33. Wei X, Decker JM, Wang S, Hui H, Kappes JC, Wu X, Salazar-Gonzalez JF, Salazar MG, Kilby JM, Saag MS, Komarova NL, Nowak MA, Hahn BH, Kwong PD, Shaw GM. 2003. Antibody neutralization and escape by HIV-1. Nature 422:307-12.

34. Decker JM, Bibollet-Ruche F, Wei X, Wang S, Levy DN, Wang W, Delaporte E, Peeters M, Derdeyn CA, Allen S, Hunter E, Saag MS, Hoxie JA, Hahn BH, Kwong PD, Robinson JE, Shaw GM. 2005. Antigenic conservation and immunogenicity of the HIV coreceptor binding site. J Exp Med 201:1407-19.

bioRxiv preprint doi: https://doi.org/10.1101/2022.12.01.518799; this version posted December 2, 2022. The copyright holder for this preprint (which was not certified by peer review) is the author/funder, who has granted bioRxiv a license to display the preprint in perpetuity. It is made available under aCC-BY-NC-ND 4.0 International license.

35. Alsahafi N, Bakouche N, Kazemi M, Richard J, Ding S, Bhattacharyya S, Das D, Anand SP, Prevost J, Tolbert WD, Lu H, Medjahed H, Gendron-Lepage G, Ortega Delgado GG, Kirk S, Melillo B, Mothes W, Sodroski J, Smith AB, 3rd, Kaufmann DE, Wu X, Pazgier M, Rouiller I, Finzi A, Munro JB. 2019. An asymmetric opening of HIV-1 envelope mediates antibody-dependent cellular cytotoxicity. Cell Host Microbe 25:578-587 e5.

36. Labrijn AF, Poignard P, Raja A, Zwick MB, Delgado K, Franti M, Binley J, Vivona V, Grundner C, Huang CC, Venturi M, Petropoulos CJ, Wrin T, Dimitrov DS, Robinson J, Kwong PD, Wyatt RT, Sodroski J, Burton DR. 2003. Access of antibody molecules to the conserved coreceptor binding site on glycoprotein gp120 is sterically restricted on primary human immunodeficiency virus type 1. J Virol 77:10557-65.

37. Moore PL, Ranchobe N, Lambson BE, Gray ES, Cave E, Abrahams MR, Bandawe G, Mlisana K, Abdool Karim SS, Williamson C, Morris L, Study C, Immunology NCfHAV. 2009. Limited neutralizing antibody specificities drive neutralization escape in early HIV-1 subtype C infection. PLoS Pathog 5:e1000598.

38. Zou S, Zhang S, Gaffney A, Ding H, Lu M, Grover JR, Farrell M, Nguyen HT, Zhao C, Anang S, Zhao M, Mohammadi M, Blanchard SC, Abrams C, Madani N, Mothes W, Kappes JC, Smith AB, 3rd, Sodroski J. 2020. Long-acting BMS-378806 analogues stabilize the State-1 conformation of the human immunodeficiency virus type 1 envelope glycoproteins. J Virol 94:e00148-20.

39. Zhang S, Wang K, Wang WL, Nguyen HT, Chen S, Lu M, Go EP, Ding H, Steinbock RT, Desaire H, Kappes JC, Sodroski J, Mao Y. 2021. Asymmetric structures and conformational plasticity of the uncleaved full-length human immunodeficiency virus envelope glycoprotein trimer. J Virol 95:e0052921.

40. Haim H, Salas I, Sodroski J. 2013. Proteolytic processing of the human immunodeficiency virus envelope glycoprotein precursor decreases conformational flexibility. J Virol 87:1884-9.

41. Herrera C, Klasse PJ, Michael E, Kake S, Barnes K, Kibler CW, Campbell-Gardener L, Si Z, Sodroski J, Moore JP, Beddows S. 2005. The impact of envelope glycoprotein cleavage on the antigenicity, infectivity, and neutralization sensitivity of Env-pseudotyped human immunodeficiency virus type 1 particles. Virology 338:154-72.

42. Pancera M, Wyatt R. 2005. Selective recognition of oligomeric HIV-1 primary isolate envelope glycoproteins by potently neutralizing ligands requires efficient precursor cleavage. Virology 332:145-56.

43. Chakrabarti BK, Pancera M, Phogat S, O'Dell S, McKee K, Guenaga J, Robinson J, Mascola J, Wyatt RT. 2011. HIV type 1 Env precursor cleavage state affects

bioRxiv preprint doi: https://doi.org/10.1101/2022.12.01.518799; this version posted December 2, 2022. The copyright holder for this preprint (which was not certified by peer review) is the author/funder, who has granted bioRxiv a license to display the preprint in perpetuity. It is made available under aCC-BY-NC-ND 4.0 International license.

recognition by both neutralizing and nonneutralizing gp41 antibodies. AIDS Res Hum Retroviruses 27:877-87.

44. Chakrabarti BK, Walker LM, Guenaga JF, Ghobbeh A, Poignard P, Burton DR, Wyatt RT. 2011. Direct antibody access to the HIV-1 membrane-proximal external region positively correlates with neutralization sensitivity. J Virol 85:8217-26.

45. Li Y, O'Dell S, Wilson R, Wu X, Schmidt SD, Hogerkorp CM, Louder MK, Longo NS, Poulsen C, Guenaga J, Chakrabarti BK, Doria-Rose N, Roederer M, Connors M, Mascola JR, Wyatt RT. 2012. HIV-1 neutralizing antibodies display dual recognition of the primary and coreceptor binding sites and preferential binding to fully cleaved envelope glycoproteins. J Virol 86:11231-41.

46. Guttman M, Cupo A, Julien JP, Sanders RW, Wilson IA, Moore JP, Lee KK. 2015. Antibody potency relates to the ability to recognize the closed, pre-fusion form of HIV Env. Nat Commun 6:6144.

47. Kwong PD, Doyle ML, Casper DJ, Cicala C, Leavitt SA, Majeed S, Steenbeke TD, Venturi M, Chaiken I, Fung M, Katinger H, Parren PW, Robinson J, Van Ryk D, Wang L, Burton DR, Freire E, Wyatt R, Sodroski J, Hendrickson WA, Arthos J. 2002. HIV-1 evades antibody-mediated neutralization through conformational masking of receptor-binding sites. Nature 420:678-82.

48. Wang Q, Finzi A, Sodroski J. 2020. The conformational states of the HIV-1 envelope glycoproteins. Trends Microbiol 28:655-667.

49. Haim H, Salas I, McGee K, Eichelberger N, Winter E, Pacheco B, Sodroski J. 2013. Modeling virus- and antibody-specific factors to predict human immunodeficiency virus neutralization efficiency. Cell Host Microbe 14:547-58.

50. Wibmer CK, Bhiman JN, Gray ES, Tumba N, Abdool Karim SS, Williamson C, Morris L, Moore PL. 2013. Viral escape from HIV-1 neutralizing antibodies drives increased plasma neutralization breadth through sequential recognition of multiple epitopes and immunotypes. PLoS Pathog 9:e1003738.

51. Gray ES, Taylor N, Wycuff D, Moore PL, Tomaras GD, Wibmer CK, Puren A, DeCamp A, Gilbert PB, Wood B, Montefiori DC, Binley JM, Shaw GM, Haynes BF, Mascola JR, Morris L. 2009. Antibody specificities associated with neutralization breadth in plasma from human immunodeficiency virus type 1 subtype C-infected blood donors. J Virol 83:8925-37.

52. Sather DN, Armann J, Ching LK, Mavrantoni A, Sellhorn G, Caldwell Z, Yu X, Wood B, Self S, Kalams S, Stamatatos L. 2009. Factors associated with the development of cross-reactive neutralizing antibodies during human immunodeficiency virus type 1 infection. J Virol 83:757-69.

bioRxiv preprint doi: https://doi.org/10.1101/2022.12.01.518799; this version posted December 2, 2022. The copyright holder for this preprint (which was not certified by peer review) is the author/funder, who has granted bioRxiv a license to display the preprint in perpetuity. It is made available under aCC-BY-NC-ND 4.0 International license.

53. Klein F, Diskin R, Scheid JF, Gaebler C, Mouquet H, Georgiev IS, Pancera M, Zhou T, Incesu RB, Fu BZ, Gnanapragasam PN, Oliveira TY, Seaman MS, Kwong PD, Bjorkman PJ, Nussenzweig MC. 2013. Somatic mutations of the immunoglobulin framework are generally required for broad and potent HIV-1 neutralization. Cell 153:126-38.

54. Walker LM, Simek MD, Priddy F, Gach JS, Wagner D, Zwick MB, Phogat SK, Poignard P, Burton DR. 2010. A limited number of antibody specificities mediate broad and potent serum neutralization in selected HIV-1 infected individuals. PLoS Pathog 6:e1001028.

55. Gray ES, Madiga MC, Hermanus T, Moore PL, Wibmer CK, Tumba NL, Werner L, Mlisana K, Sibeko S, Williamson C, Abdool Karim SS, Morris L, Team CS. 2011. The neutralization breadth of HIV-1 develops incrementally over four years and is associated with CD4+ T cell decline and high viral load during acute infection. J Virol 85:4828-40.

56. Corti D, Langedijk JP, Hinz A, Seaman MS, Vanzetta F, Fernandez-Rodriguez BM, Silacci C, Pinna D, Jarrossay D, Balla-Jhagjhoorsingh S, Willems B, Zekveld MJ, Dreja H, O'Sullivan E, Pade C, Orkin C, Jeffs SA, Montefiori DC, Davis D, Weissenhorn W, McKnight A, Heeney JL, Sallusto F, Sattentau QJ, Weiss RA, Lanzavecchia A. 2010. Analysis of memory B cell responses and isolation of novel monoclonal antibodies with neutralizing breadth from HIV-1-infected individuals. PLoS One 5:e8805.

57. Wu X, Zhou T, Zhu J, Zhang B, Georgiev I, Wang C, Chen X, Longo NS, Louder M, McKee K, O'Dell S, Perfetto S, Schmidt SD, Shi W, Wu L, Yang Y, Yang ZY, Yang Z, Zhang Z, Bonsignori M, Crump JA, Kapiga SH, Sam NE, Haynes BF, Simek M, Burton DR, Koff WC, Doria-Rose NA, Connors M, Program NCS, Mullikin JC, Nabel GJ, Roederer M, Shapiro L, Kwong PD, Mascola JR. 2011. Focused evolution of HIV-1 neutralizing antibodies revealed by structures and deep sequencing. Science 333:1593-602.

58. Hraber P, Seaman MS, Bailer RT, Mascola JR, Montefiori DC, Korber BT. 2014. Prevalence of broadly neutralizing antibody responses during chronic HIV-1 infection. AIDS 28:163-9.

59. Hessell AJ, Poignard P, Hunter M, Hangartner L, Tehrani DM, Bleeker WK, Parren PW, Marx PA, Burton DR. 2009. Effective, low-titer antibody protection against low-dose repeated mucosal SHIV challenge in macaques. Nat Med 15:951-4.

60. Mascola JR, Lewis MG, Stiegler G, Harris D, VanCott TC, Hayes D, Louder MK, Brown CR, Sapan CV, Frankel SS, Lu Y, Robb ML, Katinger H, Birx DL. 1999. Protection of macaques against pathogenic simian/human immunodeficiency virus 89.6PD by passive transfer of neutralizing antibodies. J Virol 73:4009-18.

bioRxiv preprint doi: https://doi.org/10.1101/2022.12.01.518799; this version posted December 2, 2022. The copyright holder for this preprint (which was not certified by peer review) is the author/funder, who has granted bioRxiv a license to display the preprint in perpetuity. It is made available under aCC-BY-NC-ND 4.0 International license.

61. Mascola JR, Stiegler G, VanCott TC, Katinger H, Carpenter CB, Hanson CE, Beary H, Hayes D, Frankel SS, Birx DL, Lewis MG. 2000. Protection of macaques against vaginal transmission of a pathogenic HIV-1/SIV chimeric virus by passive infusion of neutralizing antibodies. Nat Med 6:207-10.

62. Moldt B, Rakasz EG, Schultz N, Chan-Hui PY, Swiderek K, Weisgrau KL, Piaskowski SM, Bergman Z, Watkins DI, Poignard P, Burton DR. 2012. Highly potent HIV-specific antibody neutralization in vitro translates into effective protection against mucosal SHIV challenge in vivo. Proc Natl Acad Sci U S A 109:18921-5.

63. Parren PW, Marx PA, Hessell AJ, Luckay A, Harouse J, Cheng-Mayer C, Moore JP, Burton DR. 2001. Antibody protects macaques against vaginal challenge with a pathogenic R5 simian/human immunodeficiency virus at serum levels giving complete neutralization in vitro. J Virol 75:8340-7.

64. Pauthner MG, Nkolola JP, Havenar-Daughton C, Murrell B, Reiss SM, Bastidas R, Prevost J, Nedellec R, von Bredow B, Abbink P, Cottrell CA, Kulp DW, Tokatlian T, Nogal B, Bianchi M, Li H, Lee JH, Butera ST, Evans DT, Hangartner L, Finzi A, Wilson IA, Wyatt RT, Irvine DJ, Schief WR, Ward AB, Sanders RW, Crotty S, Shaw GM, Barouch DH, Burton DR. 2019. Vaccine-induced protection from homologous Tier 2 SHIV challenge in nonhuman primates depends on serum-neutralizing antibody titers. Immunity 50:241-252 e6.

65. Pauthner M, Havenar-Daughton C, Sok D, Nkolola JP, Bastidas R, Boopathy AV, Carnathan DG, Chandrashekar A, Cirelli KM, Cottrell CA, Eroshkin AM, Guenaga J, Kaushik K, Kulp DW, Liu J, McCoy LE, Oom AL, Ozorowski G, Post KW, Sharma SK, Steichen JM, de Taeye SW, Tokatlian T, Torrents de la Pena A, Butera ST, LaBranche CC, Montefiori DC, Silvestri G, Wilson IA, Irvine DJ, Sanders RW, Schief WR, Ward AB, Wyatt RT, Barouch DH, Crotty S, Burton DR. 2017. Elicitation of robust Tier 2 neutralizing antibody responses in nonhuman primates by HIV envelope trimer immunization using optimized approaches. Immunity 46:1073-1088 e6.

66. Torrents de la Pena A, de Taeye SW, Sliepen K, LaBranche CC, Burger JA, Schermer EE, Montefiori DC, Moore JP, Klasse PJ, Sanders RW. 2018. Immunogenicity in Rabbits of HIV-1 SOSIP Trimers from Clades A, B, and C, given individually, sequentially, or in combination. J Virol 92:e01957-17.

67. Klasse PJ, LaBranche CC, Ketas TJ, Ozorowski G, Cupo A, Pugach P, Ringe RP, Golabek M, van Gils MJ, Guttman M, Lee KK, Wilson IA, Butera ST, Ward AB, Montefiori DC, Sanders RW, Moore JP. 2016. Sequential and simultaneous immunization of rabbits with HIV-1 envelope glycoprotein SOSIP.664 trimers from Clades A, B and C. PLoS Pathog 12:e1005864.

68. Hu JK, Crampton JC, Cupo A, Ketas T, van Gils MJ, Sliepen K, de Taeye SW, Sok D, Ozorowski G, Deresa I, Stanfield R, Ward AB, Burton DR, Klasse PJ,

bioRxiv preprint doi: https://doi.org/10.1101/2022.12.01.518799; this version posted December 2, 2022. The copyright holder for this preprint (which was not certified by peer review) is the author/funder, who has granted bioRxiv a license to display the preprint in perpetuity. It is made available under aCC-BY-NC-ND 4.0 International license.

Sanders RW, Moore JP, Crotty S. 2015. Murine antibody responses to cleaved soluble HIV-1 envelope trimers are highly restricted in specificity. J Virol 89:10383-98.

69. Feng Y, Tran K, Bale S, Kumar S, Guenaga J, Wilson R, de Val N, Arendt H, DeStefano J, Ward AB, Wyatt RT. 2016. Thermostability of well-ordered HIV spikes correlates with the elicitation of autologous Tier 2 neutralizing antibodies. PLoS Pathog 12:e1005767.

70. Dubrovskaya V, Tran K, Ozorowski G, Guenaga J, Wilson R, Bale S, Cottrell CA, Turner HL, Seabright G, O'Dell S, Torres JL, Yang L, Feng Y, Leaman DP, Vazquez Bernat N, Liban T, Louder M, McKee K, Bailer RT, Movsesyan A, Doria-Rose NA, Pancera M, Karlsson Hedestam GB, Zwick MB, Crispin M, Mascola JR, Ward AB, Wyatt RT. 2019. Vaccination with glycan-modified HIV NFL envelope trimer-liposomes elicits broadly neutralizing antibodies to multiple sites of vulnerability. Immunity 51:915-929 e7.

71. Xu K, Acharya P, Kong R, Cheng C, Chuang GY, Liu K, Louder MK, O'Dell S, Rawi R, Sastry M, Shen CH, Zhang B, Zhou T, Asokan M, Bailer RT, Chambers M, Chen X, Choi CW, Dandey VP, Doria-Rose NA, Druz A, Eng ET, Farney SK, Foulds KE, Geng H, Georgiev IS, Gorman J, Hill KR, Jafari AJ, Kwon YD, Lai YT, Lemmin T, McKee K, Ohr TY, Ou L, Peng D, Rowshan AP, Sheng Z, Todd JP, Tsybovsky Y, Viox EG, Wang Y, Wei H, Yang Y, Zhou AF, Chen R, Yang L, Scorpio DG, McDermott AB, Shapiro L, et al. 2018. Epitope-based vaccine design yields fusion peptide-directed antibodies that neutralize diverse strains of HIV-1. Nat Med 24:857-867.

72. Sanders RW, van Gils MJ, Derking R, Sok D, Ketas TJ, Burger JA, Ozorowski G, Cupo A, Simonich C, Goo L, Arendt H, Kim HJ, Lee JH, Pugach P, Williams M, Debnath G, Moldt B, van Breemen MJ, Isik G, Medina-Ramirez M, Back JW, Koff WC, Julien JP, Rakasz EG, Seaman MS, Guttman M, Lee KK, Klasse PJ, LaBranche C, Schief WR, Wilson IA, Overbaugh J, Burton DR, Ward AB, Montefiori DC, Dean H, Moore JP. 2015. HIV-1 VACCINES. HIV-1 neutralizing antibodies induced by native-like envelope trimers. Science 349:aac4223.

73. de Taeye SW, Ozorowski G, Torrents de la Pena A, Guttman M, Julien JP, van den Kerkhof TL, Burger JA, Pritchard LK, Pugach P, Yasmeen A, Crampton J, Hu J, Bontjer I, Torres JL, Arendt H, DeStefano J, Koff WC, Schuitemaker H, Eggink D, Berkhout B, Dean H, LaBranche C, Crotty S, Crispin M, Montefiori DC, Klasse PJ, Lee KK, Moore JP, Wilson IA, Ward AB, Sanders RW. 2015. Immunogenicity of stabilized HIV-1 envelope trimers with reduced exposure of non-neutralizing epitopes. Cell 163:1702-15.

74. Kong R, Duan H, Sheng Z, Xu K, Acharya P, Chen X, Cheng C, Dingens AS, Gorman J, Sastry M, Shen CH, Zhang B, Zhou T, Chuang GY, Chao CW, Gu Y, Jafari AJ, Louder MK, O'Dell S, Rowshan AP, Viox EG, Wang Y, Choi CW, Corcoran MM, Corrigan AR, Dandey VP, Eng ET, Geng H, Foulds KE, Guo Y,

bioRxiv preprint doi: https://doi.org/10.1101/2022.12.01.518799; this version posted December 2, 2022. The copyright holder for this preprint (which was not certified by peer review) is the author/funder, who has granted bioRxiv a license to display the preprint in perpetuity. It is made available under aCC-BY-NC-ND 4.0 International license.

Kwon YD, Lin B, Liu K, Mason RD, Nason MC, Ohr TY, Ou L, Rawi R, Sarfo EK, Schon A, Todd JP, Wang S, Wei H, Wu W, Program NCS, Mullikin JC, Bailer RT, Doria-Rose NA, Karlsson Hedestam GB, Scorpio DG, et al. 2019. Antibody lineages with vaccine-induced antigen-binding hotspots develop broad HIV neutralization. Cell 178:567-584 e19.

75. Chuang GY, Lai YT, Boyington JC, Cheng C, Geng H, Narpala S, Rawi R, Schmidt SD, Tsybovsky Y, Verardi R, Xu K, Yang Y, Zhang B, Chambers M, Changela A, Corrigan AR, Kong R, Olia AS, Ou L, Sarfo EK, Wang S, Wu W, Doria-Rose NA, McDermott AB, Mascola JR, Kwong PD. 2020. Development of a 3Mut-apex-stabilized envelope trimer that expands HIV-1 neutralization breadth when used to boost fusion peptide-directed vaccine-elicited responses. J Virol 94:e00074-20.

76. Ringe RP, Pugach P, Cottrell CA, LaBranche CC, Seabright GE, Ketas TJ, Ozorowski G, Kumar S, Schorcht A, van Gils MJ, Crispin M, Montefiori DC, Wilson IA, Ward AB, Sanders RW, Klasse PJ, Moore JP. 2019. Closing and opening holes in the glycan shield of HIV-1 envelope glycoprotein SOSIP trimers can redirect the neutralizing antibody response to the newly unmasked epitopes. J Virol 93:e01656-18.

77. Charles TP, Burton SL, Arunachalam PS, Cottrell CA, Sewall LM, Bollimpelli VS, Gangadhara S, Dey AK, Ward AB, Shaw GM, Hunter E, Amara RR, Pulendran B, van Gils MJ, Derdeyn CA. 2021. The C3/465 glycan hole cluster in BG505 HIV-1 envelope is the major neutralizing target involved in preventing mucosal SHIV infection. PLoS Pathog 17:e1009257.

78. McCoy LE, van Gils MJ, Ozorowski G, Messmer T, Briney B, Voss JE, Kulp DW, Macauley MS, Sok D, Pauthner M, Menis S, Cottrell CA, Torres JL, Hsueh J, Schief WR, Wilson IA, Ward AB, Sanders RW, Burton DR. 2016. Holes in the glycan shield of the native HIV envelope are a target of trimer-elicited neutralizing antibodies. Cell Rep 16:2327-38.

79. Nogal B, Bianchi M, Cottrell CA, Kirchdoerfer RN, Sewall LM, Turner HL, Zhao F, Sok D, Burton DR, Hangartner L, Ward AB. 2020. Mapping polyclonal antibody responses in non-human primates vaccinated with HIV Env trimer subunit vaccines. Cell Rep 30:3755-3765 e7.

80. Klasse PJ, Ketas TJ, Cottrell CA, Ozorowski G, Debnath G, Camara D, Francomano E, Pugach P, Ringe RP, LaBranche CC, van Gils MJ, Bricault CA, Barouch DH, Crotty S, Silvestri G, Kasturi S, Pulendran B, Wilson IA, Montefiori DC, Sanders RW, Ward AB, Moore JP. 2018. Epitopes for neutralizing antibodies induced by HIV-1 envelope glycoprotein BG505 SOSIP trimers in rabbits and macaques. PLoS Pathog 14:e1006913.

81. Aljedani SS, Liban TJ, Tran K, Phad G, Singh S, Dubrovskaya V, Pushparaj P, Martinez-Murillo P, Rodarte J, Mileant A, Mangala Prasad V, Kinzelman R, O'Dell

bioRxiv preprint doi: https://doi.org/10.1101/2022.12.01.518799; this version posted December 2, 2022. The copyright holder for this preprint (which was not certified by peer review) is the author/funder, who has granted bioRxiv a license to display the preprint in perpetuity. It is made available under aCC-BY-NC-ND 4.0 International license.

S, Mascola JR, Lee KK, Karlsson Hedestam GB, Wyatt RT, Pancera M. 2021. Structurally related but genetically unrelated antibody lineages converge on an immunodominant HIV-1 Env neutralizing determinant following trimer immunization. PLoS Pathog 17:e1009543.

82. Lei L, Yang YR, Tran K, Wang Y, Chiang CI, Ozorowski G, Xiao Y, Ward AB, Wyatt RT, Li Y. 2019. The HIV-1 envelope glycoprotein C3/V4 region defines a prevalent neutralization epitope following immunization. Cell Rep 27:586-598 e6.

83. van Schooten J, van Haaren MM, Li H, McCoy LE, Havenar-Daughton C, Cottrell CA, Burger JA, van der Woude P, Helgers LC, Tomris I, Labranche CC, Montefiori DC, Ward AB, Burton DR, Moore JP, Sanders RW, Crotty S, Shaw GM, van Gils MJ. 2021. Antibody responses induced by SHIV infection are more focused than those induced by soluble native HIV-1 envelope trimers in non-human primates. PLoS Pathog 17:e1009736.

84. Antanasijevic A, Sewall LM, Cottrell CA, Carnathan DG, Jimenez LE, Ngo JT, Silverman JB, Groschel B, Georgeson E, Bhiman J, Bastidas R, LaBranche C, Allen JD, Copps J, Perrett HR, Rantalainen K, Cannac F, Yang YR, de la Pena AT, Rocha RF, Berndsen ZT, Baker D, King NP, Sanders RW, Moore JP, Crotty S, Crispin M, Montefiori DC, Burton DR, Schief WR, Silvestri G, Ward AB. 2021. Polyclonal antibody responses to HIV Env immunogens resolved using cryoEM. Nat Commun 12:4817.

85. Sanders RW, Derking R, Cupo A, Julien JP, Yasmeen A, de Val N, Kim HJ, Blattner C, de la Pena AT, Korzun J, Golabek M, de Los Reyes K, Ketas TJ, van Gils MJ, King CR, Wilson IA, Ward AB, Klasse PJ, Moore JP. 2013. A next-generation cleaved, soluble HIV-1 Env trimer, BG505 SOSIP.664 gp140, expresses multiple epitopes for broadly neutralizing but not non-neutralizing antibodies. PLoS Pathog 9:e1003618.

86. Alsahafi N, Debbeche O, Sodroski J, Finzi A. 2015. Effects of the I559P gp41 change on the conformation and function of the human immunodeficiency virus (HIV-1) membrane envelope glycoprotein trimer. PLoS One 10:e0122111.

87. Alsahafi N, Anand SP, Castillo-Menendez L, Verly MM, Medjahed H, Prevost J, Herschhorn A, Richard J, Schon A, Melillo B, Freire E, Smith AB, 3rd, Sodroski J, Finzi A. 2018. SOSIP changes affect human immunodeficiency virus type 1 envelope glycoprotein conformation and CD4 engagement. J Virol 92.

88. Castillo-Menendez LR, Nguyen HT, Sodroski J. 2019. Conformational differences between functional human immunodeficiency virus envelope glycoprotein trimers and stabilized soluble trimers. J Virol 93:e01709-18.

89. Nguyen HT, Alsahafi N, Finzi A, Sodroski JG. 2019. Effects of the SOS (A501C/T605C) and DS (I201C/A433C) disulfide bonds on HIV-1 membrane envelope glycoprotein conformation and function. J Virol 93:e00304-19.

bioRxiv preprint doi: https://doi.org/10.1101/2022.12.01.518799; this version posted December 2, 2022. The copyright holder for this preprint (which was not certified by peer review) is the author/funder, who has granted bioRxiv a license to display the preprint in perpetuity. It is made available under aCC-BY-NC-ND 4.0 International license.

90. Go EP, Herschhorn A, Gu C, Castillo-Menendez L, Zhang S, Mao Y, Chen H, Ding H, Wakefield JK, Hua D, Liao HX, Kappes JC, Sodroski J, Desaire H. 2015. Comparative analysis of the glycosylation profiles of membrane-anchored HIV-1 envelope glycoprotein trimers and soluble gp140. J Virol 89:8245-57.

91. Cao L, Pauthner M, Andrabi R, Rantalainen K, Berndsen Z, Diedrich JK, Menis S, Sok D, Bastidas R, Park SR, Delahunty CM, He L, Guenaga J, Wyatt RT, Schief WR, Ward AB, Yates JR, 3rd, Burton DR, Paulson JC. 2018. Differential processing of HIV envelope glycans on the virus and soluble recombinant trimer. Nat Commun 9:3693.

92. Torrents de la Pena A, Rantalainen K, Cottrell CA, Allen JD, van Gils MJ, Torres JL, Crispin M, Sanders RW, Ward AB. 2019. Similarities and differences between native HIV-1 envelope glycoprotein trimers and stabilized soluble trimer mimetics. PLoS Pathog 15:e1007920.

93. Struwe WB, Chertova E, Allen JD, Seabright GE, Watanabe Y, Harvey DJ, Medina-Ramirez M, Roser JD, Smith R, Westcott D, Keele BF, Bess JW, Jr., Sanders RW, Lifson JD, Moore JP, Crispin M. 2018. Site-specific glycosylation of virion-derived HIV-1 Env is mimicked by a soluble trimeric immunogen. Cell Rep 24:1958-1966 e5.

94. Castillo-Menendez LR, Witt K, Espy N, Princiotto A, Madani N, Pacheco B, Finzi A, Sodroski J. 2018. Comparison of uncleaved and mature human immunodeficiency virus membrane envelope glycoprotein trimers. J Virol 92:e00277-18.

95. Lu M, Ma X, Castillo-Menendez LR, Gorman J, Alsahafi N, Ermel U, Terry DS, Chambers M, Peng D, Zhang B, Zhou T, Reichard N, Wang K, Grover JR, Carman BP, Gardner MR, Nikic-Spiegel I, Sugawara A, Arthos J, Lemke EA, Smith AB, 3rd, Farzan M, Abrams C, Munro JB, McDermott AB, Finzi A, Kwong PD, Blanchard SC, Sodroski JG, Mothes W. 2019. Associating HIV-1 envelope glycoprotein structures with states on the virus observed by smFRET. Nature 568:415-419.

96. Mangala Prasad V, Leaman DP, Lovendahl KN, Croft JT, Benhaim MA, Hodge EA, Zwick MB, Lee KK. 2022. Cryo-ET of Env on intact HIV virions reveals structural variation and positioning on the Gag lattice. Cell 185:641-653 e17.

97. McCoy LE, Burton DR. 2017. Identification and specificity of broadly neutralizing antibodies against HIV. Immunol Rev 275:11-20.

98. Haynes BF, Burton DR, Mascola JR. 2019. Multiple roles for HIV broadly neutralizing antibodies. Sci Transl Med 11:eaaz2686.

99. Haynes BF, Verkoczy L. 2014. AIDS/HIV. Host controls of HIV neutralizing

bioRxiv preprint doi: https://doi.org/10.1101/2022.12.01.518799; this version posted December 2, 2022. The copyright holder for this preprint (which was not certified by peer review) is the author/funder, who has granted bioRxiv a license to display the preprint in perpetuity. It is made available under aCC-BY-NC-ND 4.0 International license.

antibodies. Science 344:588-9.

100. Haynes BF, Kelsoe G, Harrison SC, Kepler TB. 2012. B-cell-lineage immunogen design in vaccine development with HIV-1 as a case study. Nat Biotechnol 30:423-33.

101. Seabright GE, Doores KJ, Burton DR, Crispin M. 2019. Protein and Glycan Mimicry in HIV Vaccine Design. J Mol Biol 431:2223-2247.

102. Liu H, Su X, Si L, Lu L, Jiang S. 2018. The development of HIV vaccines targeting gp41 membrane-proximal external region (MPER): challenges and prospects. Protein Cell 9:596-615.

103. Ofek G, Tang M, Sambor A, Katinger H, Mascola JR, Wyatt R, Kwong PD. 2004. Structure and mechanistic analysis of the anti-human immunodeficiency virus type 1 antibody 2F5 in complex with its gp41 epitope. J Virol 78:10724-37.

104. Irimia A, Serra AM, Sarkar A, Jacak R, Kalyuzhniy O, Sok D, Saye-Francisco KL, Schiffner T, Tingle R, Kubitz M, Adachi Y, Stanfield RL, Deller MC, Burton DR, Schief WR, Wilson IA. 2017. Lipid interactions and angle of approach to the HIV-1 viral membrane of broadly neutralizing antibody 10E8: Insights for vaccine and therapeutic design. PLoS Pathog 13:e1006212.

105. Rantalainen K, Berndsen ZT, Antanasijevic A, Schiffner T, Zhang X, Lee WH, Torres JL, Zhang L, Irimia A, Copps J, Zhou KH, Kwon YD, Law WH, Schramm CA, Verardi R, Krebs SJ, Kwong PD, Doria-Rose NA, Wilson IA, Zwick MB, Yates JR, 3rd, Schief WR, Ward AB. 2020. HIV-1 envelope and MPER antibody structures in lipid assemblies. Cell Rep 31:107583.

106. Huang J, Ofek G, Laub L, Louder MK, Doria-Rose NA, Longo NS, Imamichi H, Bailer RT, Chakrabarti B, Sharma SK, Alam SM, Wang T, Yang Y, Zhang B, Migueles SA, Wyatt R, Haynes BF, Kwong PD, Mascola JR, Connors M. 2012. Broad and potent neutralization of HIV-1 by a gp41-specific human antibody. Nature 491:406-12.

107. Haim H, Strack B, Kassa A, Madani N, Wang L, Courter JR, Princiotto A, McGee K, Pacheco B, Seaman MS, Smith AB, 3rd, Sodroski J. 2011. Contribution of intrinsic reactivity of the HIV-1 envelope glycoproteins to CD4-independent infection and global inhibitor sensitivity. PLoS Pathog 7:e1002101.

108. Bradley T, Trama A, Tumba N, Gray E, Lu X, Madani N, Jahanbakhsh F, Eaton A, Xia SM, Parks R, Lloyd KE, Sutherland LL, Scearce RM, Bowman CM, Barnett S, Abdool-Karim SS, Boyd SD, Melillo B, Smith AB, 3rd, Sodroski J, Kepler TB, Alam SM, Gao F, Bonsignori M, Liao HX, Moody MA, Montefiori D, Santra S, Morris L, Haynes BF. 2016. Amino acid changes in the HIV-1 gp41 membrane proximal region control virus neutralization sensitivity. EBioMedicine 12:196-207.

bioRxiv preprint doi: https://doi.org/10.1101/2022.12.01.518799; this version posted December 2, 2022. The copyright holder for this preprint (which was not certified by peer review) is the author/funder, who has granted bioRxiv a license to display the preprint in perpetuity. It is made available under aCC-BY-NC-ND 4.0 International license.

109. Ringe R, Bhattacharya J. 2012. Association of enhanced HIV-1 neutralization by a single Y681H substitution in gp41 with increased gp120-CD4 interaction and macrophage infectivity. PLoS One 7:e37157.

110. Blish CA, Nguyen MA, Overbaugh J. 2008. Enhancing exposure of HIV-1 neutralization epitopes through mutations in gp41. PLoS Med 5:e9.

111. Lovelace E, Xu H, Blish CA, Strong R, Overbaugh J. 2011. The role of amino acid changes in the human immunodeficiency virus type 1 transmembrane domain in antibody binding and neutralization. Virology 421:235-44.

112. Salimi H, Johnson J, Flores MG, Zhang MS, O'Malley Y, Houtman JC, Schlievert PM, Haim H. 2020. The lipid membrane of HIV-1 stabilizes the viral envelope glycoproteins and modulates their sensitivity to antibody neutralization. J Biol Chem 295:348-362.

113. Wang Q, Esnault F, Zhao M, Chiu TJ, Smith AB, 3rd, Nguyen HT, Sodroski JG. 2022. Global increases in human immunodeficiency virus neutralization sensitivity due to alterations in the membrane-proximal external region of the envelope glycoprotein can be minimized by distant State 1-stabilizing changes. J Virol 96:e0187821.

114. Julien JP, Cupo A, Sok D, Stanfield RL, Lyumkis D, Deller MC, Klasse PJ, Burton DR, Sanders RW, Moore JP, Ward AB, Wilson IA. 2013. Crystal structure of a soluble cleaved HIV-1 envelope trimer. Science 342:1477-83.

115. Lyumkis D, Julien JP, de Val N, Cupo A, Potter CS, Klasse PJ, Burton DR, Sanders RW, Moore JP, Carragher B, Wilson IA, Ward AB. 2013. Cryo-EM structure of a fully glycosylated soluble cleaved HIV-1 envelope trimer. Science 342:1484-90.

116. Pancera M, Zhou T, Druz A, Georgiev IS, Soto C, Gorman J, Huang J, Acharya P, Chuang GY, Ofek G, Stewart-Jones GB, Stuckey J, Bailer RT, Joyce MG, Louder MK, Tumba N, Yang Y, Zhang B, Cohen MS, Haynes BF, Mascola JR, Morris L, Munro JB, Blanchard SC, Mothes W, Connors M, Kwong PD. 2014. Structure and immune recognition of trimeric pre-fusion HIV-1 Env. Nature 514:455-61.

117. Bartesaghi A, Merk A, Borgnia MJ, Milne JL, Subramaniam S. 2013. Prefusion structure of trimeric HIV-1 envelope glycoprotein determined by cryo-electron microscopy. Nat Struct Mol Biol 20:1352-7.

118. Lu M, Ma X, Reichard N, Terry DS, Arthos J, Smith AB, 3rd, Sodroski JG, Blanchard SC, Mothes W. 2020. Shedding-resistant HIV-1 envelope glycoproteins adopt downstream conformations that remain responsive to conformation-preferring ligands. J Virol 94:e00597-20.

bioRxiv preprint doi: https://doi.org/10.1101/2022.12.01.518799; this version posted December 2, 2022. The copyright holder for this preprint (which was not certified by peer review) is the author/funder, who has granted bioRxiv a license to display the preprint in perpetuity. It is made available under aCC-BY-NC-ND 4.0 International license.

119. Chertova E, Bess JW, Jr., Crise BJ, Sowder IR, Schaden TM, Hilburn JM, Hoxie JA, Benveniste RE, Lifson JD, Henderson LE, Arthur LO. 2002. Envelope glycoprotein incorporation, not shedding of surface envelope glycoprotein (gp120/SU), is the primary determinant of SU content of purified human immunodeficiency virus type 1 and simian immunodeficiency virus. J Virol 76:5315-25.

120. Zhu P, Chertova E, Bess J, Jr., Lifson JD, Arthur LO, Liu J, Taylor KA, Roux KH. 2003. Electron tomography analysis of envelope glycoprotein trimers on HIV and simian immunodeficiency virus virions. Proc Natl Acad Sci U S A 100:15812-7.

121. Poignard P, Moulard M, Golez E, Vivona V, Franti M, Venturini S, Wang M, Parren PW, Burton DR. 2003. Heterogeneity of envelope molecules expressed on primary human immunodeficiency virus type 1 particles as probed by the binding of neutralizing and nonneutralizing antibodies. J Virol 77:353-65.

122. Hammonds J, Chen X, Fouts T, DeVico A, Montefiori D, Spearman P. 2005. Induction of neutralizing antibodies against human immunodeficiency virus type 1 primary isolates by Gag-Env pseudovirion immunization. J Virol 79:14804-14.

123. Wang BZ, Liu W, Kang SM, Alam M, Huang C, Ye L, Sun Y, Li Y, Kothe DL, Pushko P, Dokland T, Haynes BF, Smith G, Hahn BH, Compans RW. 2007. Incorporation of high levels of chimeric human immunodeficiency virus envelope glycoproteins into virus-like particles. J Virol 81:10869-78.

124. Moore PL, Crooks ET, Porter L, Zhu P, Cayanan CS, Grise H, Corcoran P, Zwick MB, Franti M, Morris L, Roux KH, Burton DR, Binley JM. 2006. Nature of nonfunctional envelope proteins on the surface of human immunodeficiency virus type 1. J Virol 80:2515-28.

125. Crooks ET, Moore PL, Franti M, Cayanan CS, Zhu P, Jiang P, de Vries RP, Wiley C, Zharkikh I, Schulke N, Roux KH, Montefiori DC, Burton DR, Binley JM. 2007. A comparative immunogenicity study of HIV-1 virus-like particles bearing various forms of envelope proteins, particles bearing no envelope and soluble monomeric gp120. Virology 366:245-62.

126. Tong T, Crooks ET, Osawa K, Robinson JE, Barnes M, Apetrei C, Binley JM. 2014. Multi-parameter exploration of HIV-1 virus-like particles as neutralizing antibody immunogens in guinea pigs, rabbits and macaques. Virology 456-457:55-69.

127. Crooks ET, Tong T, Osawa K, Binley JM. 2011. Enzyme digests eliminate nonfunctional Env from HIV-1 particle surfaces, leaving native Env trimers intact and viral infectivity unaffected. J Virol 85:5825-39.

128. Tong T, Crooks ET, Osawa K, Binley JM. 2012. HIV-1 virus-like particles bearing

bioRxiv preprint doi: https://doi.org/10.1101/2022.12.01.518799; this version posted December 2, 2022. The copyright holder for this preprint (which was not certified by peer review) is the author/funder, who has granted bioRxiv a license to display the preprint in perpetuity. It is made available under aCC-BY-NC-ND 4.0 International license.

pure env trimers expose neutralizing epitopes but occlude nonneutralizing epitopes. J Virol 86:3574-87.

129. Tong T, Osawa K, Robinson JE, Crooks ET, Binley JM. 2013. Topological analysis of HIV-1 glycoproteins expressed in situ on virus surfaces reveals tighter packing but greater conformational flexibility than for soluble gp120. J Virol 87:9233-49.

130. Crooks ET, Tong T, Chakrabarti B, Narayan K, Georgiev IS, Menis S, Huang X, Kulp D, Osawa K, Muranaka J, Stewart-Jones G, Destefano J, O'Dell S, LaBranche C, Robinson JE, Montefiori DC, McKee K, Du SX, Doria-Rose N, Kwong PD, Mascola JR, Zhu P, Schief WR, Wyatt RT, Whalen RG, Binley JM. 2015. Vaccine-elicited Tier 2 HIV-1 neutralizing antibodies bind to quaternary epitopes involving glycan-deficient patches proximal to the CD4 binding site. PLoS Pathog 11:e1004932.

131. Crooks ET, Osawa K, Tong T, Grimley SL, Dai YD, Whalen RG, Kulp DW, Menis S, Schief WR, Binley JM. 2017. Effects of partially dismantling the CD4 binding site glycan fence of HIV-1 Envelope glycoprotein trimers on neutralizing antibody induction. Virology 505:193-209.

132. Gonelli CA, Khoury G, Center RJ, Purcell DFJ. 2019. HIV-1-based virus-like particles that morphologically resemble mature, infectious HIV-1 virions. Viruses 11:507.

133. Gonelli CA, King HAD, Mackenzie C, Sonza S, Center RJ, Purcell DFJ. 2021. Immunogenicity of HIV-1-based virus-like particles with increased incorporation and stability of membrane-bound Env. Vaccines (Basel) 9:239.

134. Stano A, Leaman DP, Kim AS, Zhang L, Autin L, Ingale J, Gift SK, Truong J, Wyatt RT, Olson AJ, Zwick MB. 2017. Dense array of spikes on HIV-1 virion particles. J Virol 91:e00415-17.

135. Beltran-Pavez C, Bontjer I, Gonzalez N, Pernas M, Merino-Mansilla A, Olvera A, Miro JM, Brander C, Alcami J, Sanders RW, Sanchez-Merino V, Yuste E. 2022. Potent induction of envelope-specific antibody responses by virus-like particle immunogens based on HIV-1 envelopes from patients with early broadly neutralizing responses. J Virol 96:e01343-21.

136. Provine NM, Puryear WB, Wu X, Overbaugh J, Haigwood NL. 2009. The infectious molecular clone and pseudotyped virus models of human immunodeficiency virus type 1 exhibit significant differences in virion composition with only moderate differences in infectivity and inhibition sensitivity. J Virol 83:9002-7.

137. Hammonds J, Chen X, Ding L, Fouts T, De Vico A, zur Megede J, Barnett S, Spearman P. 2003. Gp120 stability on HIV-1 virions and Gag-Env pseudovirions

bioRxiv preprint doi: https://doi.org/10.1101/2022.12.01.518799; this version posted December 2, 2022. The copyright holder for this preprint (which was not certified by peer review) is the author/funder, who has granted bioRxiv a license to display the preprint in perpetuity. It is made available under aCC-BY-NC-ND 4.0 International license.

is enhanced by an uncleaved Gag core. Virology 314:636-49.

138. McKeating JA, McKnight A, Moore JP. 1991. Differential loss of envelope glycoprotein gp120 from virions of human immunodeficiency virus type 1 isolates: effects on infectivity and neutralization. J Virol 65:852-60.

139. Layne SP, Merges MJ, Dembo M, Spouge JL, Conley SR, Moore JP, Raina JL, Renz H, Gelderblom HR, Nara PL. 1992. Factors underlying spontaneous inactivation and susceptibility to neutralization of human immunodeficiency virus. Virology 189:695-714.

140. Sarafianos SG, Marchand B, Das K, Himmel DM, Parniak MA, Hughes SH, Arnold E. 2009. Structure and function of HIV-1 reverse transcriptase: molecular mechanisms of polymerization and inhibition. J Mol Biol 385:693-713.

141. Rice P, Craigie R, Davies DR. 1996. Retroviral integrases and their cousins. Curr Opin Struct Biol 6:76-83.

142. Vandegraaff N, Engelman A. 2007. Molecular mechanisms of HIV integration and therapeutic intervention. Expert Rev Mol Med 9:1-19.

143. Waheed AA, Ablan SD, Roser JD, Sowder RC, Schaffner CP, Chertova E, Freed EO. 2007. HIV-1 escape from the entry-inhibiting effects of a cholesterol-binding compound via cleavage of gp41 by the viral protease. Proc Natl Acad Sci U S A 104:8467-71.

144. Waheed AA, Ablan SD, Sowder RC, Roser JD, Schaffner CP, Chertova E, Freed EO. 2010. Effect of mutations in the human immunodeficiency virus type 1 protease on cleavage of the gp41 cytoplasmic tail. J Virol 84:3121-6.

145. Trkola A, Purtscher M, Muster T, Ballaun C, Buchacher A, Sullivan N, Srinivasan K, Sodroski J, Moore JP, Katinger H. 1996. Human monoclonal antibody 2G12 defines a distinctive neutralization epitope on the gp120 glycoprotein of human immunodeficiency virus type 1. J Virol 70:1100-8.

146. Wu X, Yang ZY, Li Y, Hogerkorp CM, Schief WR, Seaman MS, Zhou T, Schmidt SD, Wu L, Xu L, Longo NS, McKee K, O'Dell S, Louder MK, Wycuff DL, Feng Y, Nason M, Doria-Rose N, Connors M, Kwong PD, Roederer M, Wyatt RT, Nabel GJ, Mascola JR. 2010. Rational design of envelope identifies broadly neutralizing human monoclonal antibodies to HIV-1. Science 329:856-61.

147. Walker LM, Phogat SK, Chan-Hui PY, Wagner D, Phung P, Goss JL, Wrin T, Simek MD, Fling S, Mitcham JL, Lehrman JK, Priddy FH, Olsen OA, Frey SM, Hammond PW, Protocol GPI, Kaminsky S, Zamb T, Moyle M, Koff WC, Poignard P, Burton DR. 2009. Broad and potent neutralizing antibodies from an African donor reveal a new HIV-1 vaccine target. Science 326:285-9.

bioRxiv preprint doi: https://doi.org/10.1101/2022.12.01.518799; this version posted December 2, 2022. The copyright holder for this preprint (which was not certified by peer review) is the author/funder, who has granted bioRxiv a license to display the preprint in perpetuity. It is made available under aCC-BY-NC-ND 4.0 International license.

148. Walker LM, Huber M, Doores KJ, Falkowska E, Pejchal R, Julien JP, Wang SK, Ramos A, Chan-Hui PY, Moyle M, Mitcham JL, Hammond PW, Olsen OA, Phung P, Fling S, Wong CH, Phogat S, Wrin T, Simek MD, Protocol GPI, Koff WC, Wilson IA, Burton DR, Poignard P. 2011. Broad neutralization coverage of HIV by multiple highly potent antibodies. Nature 477:466-70.

149. Blattner C, Lee JH, Sliepen K, Derking R, Falkowska E, de la Pena AT, Cupo A, Julien JP, van Gils M, Lee PS, Peng W, Paulson JC, Poignard P, Burton DR, Moore JP, Sanders RW, Wilson IA, Ward AB. 2014. Structural delineation of a quaternary, cleavage-dependent epitope at the gp41-gp120 interface on intact HIV-1 Env trimers. Immunity 40:669-80.

150. Huang J, Kang BH, Pancera M, Lee JH, Tong T, Feng Y, Imamichi H, Georgiev IS, Chuang GY, Druz A, Doria-Rose NA, Laub L, Sliepen K, van Gils MJ, de la Pena AT, Derking R, Klasse PJ, Migueles SA, Bailer RT, Alam M, Pugach P, Haynes BF, Wyatt RT, Sanders RW, Binley JM, Ward AB, Mascola JR, Kwong PD, Connors M. 2014. Broad and potent HIV-1 neutralization by a human antibody that binds the gp41-gp120 interface. Nature 515:138-42.

151. Boots LJ, McKenna PM, Arnold BA, Keller PM, Gorny MK, Zolla-Pazner S, Robinson JE, Conley AJ. 1997. Anti-human immunodeficiency virus type 1 human monoclonal antibodies that bind discontinuous epitopes in the viral glycoproteins can identify mimotopes from recombinant phage peptide display libraries. AIDS Res Hum Retroviruses 13:1549-59.

152. Gorny MK, Conley AJ, Karwowska S, Buchbinder A, Xu JY, Emini EA, Koenig S, Zolla-Pazner S. 1992. Neutralization of diverse human immunodeficiency virus type 1 variants by an anti-V3 human monoclonal antibody. J Virol 66:7538-42.

153. Thali M, Moore JP, Furman C, Charles M, Ho DD, Robinson J, Sodroski J. 1993. Characterization of conserved human immunodeficiency virus type 1 gp120 neutralization epitopes exposed upon gp120-CD4 binding. J Virol 67:3978-88.

154. Xiang SH, Wang L, Abreu M, Huang CC, Kwong PD, Rosenberg E, Robinson JE, Sodroski J. 2003. Epitope mapping and characterization of a novel CD4-induced human monoclonal antibody capable of neutralizing primary HIV-1 strains. Virology 315:124-34.

155. Posner MR, Hideshima T, Cannon T, Mukherjee M, Mayer KH, Byrn RA. 1991. An IgG human monoclonal antibody that reacts with HIV-1/GP120, inhibits virus binding to cells, and neutralizes infection. J Immunol 146:4325-32.

156. Thali M, Olshevsky U, Furman C, Gabuzda D, Posner M, Sodroski J. 1991. Characterization of a discontinuous human immunodeficiency virus type 1 gp120 epitope recognized by a broadly reactive neutralizing human monoclonal antibody. J Virol 65:6188-93.

bioRxiv preprint doi: https://doi.org/10.1101/2022.12.01.518799; this version posted December 2, 2022. The copyright holder for this preprint (which was not certified by peer review) is the author/funder, who has granted bioRxiv a license to display the preprint in perpetuity. It is made available under aCC-BY-NC-ND 4.0 International license.

157. Madani N, Princiotto AM, Easterhoff D, Bradley T, Luo K, Williams WB, Liao HX, Moody MA, Phad GE, Vazquez Bernat N, Melillo B, Santra S, Smith AB, 3rd, Karlsson Hedestam GB, Haynes B, Sodroski J. 2016. Antibodies elicited by multiple envelope glycoprotein immunogens in primates neutralize primary human immunodeficiency viruses (HIV-1) sensitized by CD4-mimetic compounds. J Virol 90:5031-5046.

158. Cavacini LA, Emes CL, Wisnewski AV, Power J, Lewis G, Montefiori D, Posner MR. 1998. Functional and molecular characterization of human monoclonal antibody reactive with the immunodominant region of HIV type 1 glycoprotein 41. AIDS Res Hum Retroviruses 14:1271-80.

159. Rizzuto CD, Wyatt R, Hernandez-Ramos N, Sun Y, Kwong PD, Hendrickson WA, Sodroski J. 1998. A conserved HIV gp120 glycoprotein structure involved in chemokine receptor binding. Science 280:1949-53.

160. Huang CC, Tang M, Zhang MY, Majeed S, Montabana E, Stanfield RL, Dimitrov DS, Korber B, Sodroski J, Wilson IA, Wyatt R, Kwong PD. 2005. Structure of a V3-containing HIV-1 gp120 core. Science 310:1025-8.

161. Moore JP, McKeating JA, Weiss RA, Sattentau QJ. 1990. Dissociation of gp120 from HIV-1 virions induced by soluble CD4. Science 250:1139-42.

162. Lin PF, Blair W, Wang T, Spicer T, Guo Q, Zhou N, Gong YF, Wang HG, Rose R, Yamanaka G, Robinson B, Li CB, Fridell R, Deminie C, Demers G, Yang Z, Zadjura L, Meanwell N, Colonno R. 2003. A small molecule HIV-1 inhibitor that targets the HIV-1 envelope and inhibits CD4 receptor binding. Proc Natl Acad Sci U S A 100:11013-8.

163. Wang T, Zhang Z, Wallace OB, Deshpande M, Fang H, Yang Z, Zadjura LM, Tweedie DL, Huang S, Zhao F, Ranadive S, Robinson BS, Gong YF, Ricarrdi K, Spicer TP, Deminie C, Rose R, Wang HG, Blair WS, Shi PY, Lin PF, Colonno RJ, Meanwell NA. 2003. Discovery of 4-benzoyl-1-[(4-methoxy-1H- pyrrolo[2,3-b]pyridin-3-yl)oxoacetyl]-2- (R)-methylpiperazine (BMS-378806): a novel HIV-1 attachment inhibitor that interferes with CD4-gp120 interactions. J Med Chem 46:4236-9.

164. Pancera M, Shahzad-Ul-Hussan S, Doria-Rose NA, McLellan JS, Bailer RT, Dai K, Loesgen S, Louder MK, Staupe RP, Yang Y, Zhang B, Parks R, Eudailey J, Lloyd KE, Blinn J, Alam SM, Haynes BF, Amin MN, Wang LX, Burton DR, Koff WC, Nabel GJ, Mascola JR, Bewley CA, Kwong PD. 2013. Structural basis for diverse N-glycan recognition by HIV-1-neutralizing V1-V2-directed antibody PG16. Nat Struct Mol Biol 20:804-13.

165. Wlodawer A, Miller M, Jaskolski M, Sathyanarayana BK, Baldwin E, Weber IT, Selk LM, Clawson L, Schneider J, Kent SB. 1989. Conserved folding in retroviral proteases: crystal structure of a synthetic HIV-1 protease. Science 245:616-21.

bioRxiv preprint doi: https://doi.org/10.1101/2022.12.01.518799; this version posted December 2, 2022. The copyright holder for this preprint (which was not certified by peer review) is the author/funder, who has granted bioRxiv a license to display the preprint in perpetuity. It is made available under aCC-BY-NC-ND 4.0 International license.

166. Melillo B, Liang S, Park J, Schon A, Courter JR, LaLonde JM, Wendler DJ, Princiotto AM, Seaman MS, Freire E, Sodroski J, Madani N, Hendrickson WA, Smith AB, 3rd. 2016. Small-molecule CD4-mimics: structure-based optimization of HIV-1 entry inhibition. ACS Med Chem Lett 7:330-4.

167. Nguyen HT, Qualizza A, Anang S, Zhao M, Zou S, Zhou R, Wang Q, Zhang S, Deshpande A, Ding H, Chiu TJ, Smith AB, 3rd, Kappes JC, Sodroski JG. 2022. Functional and highly cross-linkable HIV-1 envelope glycoproteins enriched in a pretriggered conformation. J Virol 96:e0166821.

168. Herschhorn A, Ma X, Gu C, Ventura JD, Castillo-Menendez L, Melillo B, Terry DS, Smith AB, 3rd, Blanchard SC, Munro JB, Mothes W, Finzi A, Sodroski J. 2016. Release of gp120 restraints leads to an entry-competent intermediate state of the HIV-1 envelope glycoproteins. mBio 7:e01598-16.

169. Herschhorn A, Gu C, Moraca F, Ma X, Farrell M, Smith AB, 3rd, Pancera M, Kwong PD, Schon A, Freire E, Abrams C, Blanchard SC, Mothes W, Sodroski JG. 2017. The beta20-beta21 of gp120 is a regulatory switch for HIV-1 Env conformational transitions. Nat Commun 8:1049.

170. Gorny MK, Wang XH, Williams C, Volsky B, Revesz K, Witover B, Burda S, Urbanski M, Nyambi P, Krachmarov C, Pinter A, Zolla-Pazner S, Nadas A. 2009. Preferential use of the VH5-51 gene segment by the human immune response to code for antibodies against the V3 domain of HIV-1. Mol Immunol 46:917-26.

171. Anang S, Richard J, Bourassa C, Goyette G, Chiu TJ, Chen HC, Smith AB, 3rd, Madani N, Finzi A, Sodroski J. 2022. Characterization of human immunodeficiency virus (HIV-1) envelope glycoprotein variants selected for resistance to a CD4-mimetic compound. J Virol 96:e0063622.

172. Kassa A, Finzi A, Pancera M, Courter JR, Smith AB, 3rd, Sodroski J. 2009. Identification of a human immunodeficiency virus type 1 envelope glycoprotein variant resistant to cold inactivation. J Virol 83:4476-88.

173. Kassa A, Madani N, Schon A, Haim H, Finzi A, Xiang SH, Wang L, Princiotto A, Pancera M, Courter J, Smith AB, 3rd, Freire E, Kwong PD, Sodroski J. 2009. Transitions to and from the CD4-bound conformation are modulated by a single-residue change in the human immunodeficiency virus type 1 gp120 inner domain. J Virol 83:8364-78.

174. Krowicka H, Robinson JE, Clark R, Hager S, Broyles S, Pincus SH. 2008. Use of tissue culture cell lines to evaluate HIV antiviral resistance. AIDS Res Hum Retroviruses 24:957-67.

175. Hoxie JA. 1991. CD4 envelope interactions of HIV-1 and related human retroviruses. Adv Exp Med Biol 300:159-66.

bioRxiv preprint doi: https://doi.org/10.1101/2022.12.01.518799; this version posted December 2, 2022. The copyright holder for this preprint (which was not certified by peer review) is the author/funder, who has granted bioRxiv a license to display the preprint in perpetuity. It is made available under aCC-BY-NC-ND 4.0 International license.

176. Ding S, Gasser R, Gendron-Lepage G, Medjahed H, Tolbert WD, Sodroski J, Pazgier M, Finzi A. 2019. CD4 incorporation into HIV-1 viral particles exposes envelope epitopes recognized by CD4-induced antibodies. J Virol 93:e01403-19.

177. Liu J, Bartesaghi A, Borgnia MJ, Sapiro G, Subramaniam S. 2008. Molecular architecture of native HIV-1 gp120 trimers. Nature 455:109-13.

178. Li Z, Li W, Lu M, Bess J, Jr., Chao CW, Gorman J, Terry DS, Zhang B, Zhou T, Blanchard SC, Kwong PD, Lifson JD, Mothes W, Liu J. 2020. Subnanometer structures of HIV-1 envelope trimers on aldrithiol-2-inactivated virus particles. Nat Struct Mol Biol 27:726-734.

179. Mangala Prasad V, Leaman DP, Lovendahl KN, Croft JT, Benhaim MA, Hodge EA, Zwick MB, Lee KK. 2022. Cryo-ET of Env on intact HIV virions reveals structural variation and positioning on the Gag lattice. Cell 185:641-653 e17.

180. Agrawal N, Leaman DP, Rowcliffe E, Kinkead H, Nohria R, Akagi J, Bauer K, Du SX, Whalen RG, Burton DR, Zwick MB. 2011. Functional stability of unliganded envelope glycoprotein spikes among isolates of human immunodeficiency virus type 1 (HIV-1). PLoS One 6:e21339.

181. Chen BK, Gandhi RT, Baltimore D. 1996. CD4 down-modulation during infection of human T cells with human immunodeficiency virus type 1 involves independent activities of vpu, env, and nef. J Virol 70:6044-53.

182. Levesque K, Zhao YS, Cohen EA. 2003. Vpu exerts a positive effect on HIV-1 infectivity by down-modulating CD4 receptor molecules at the surface of HIV-1-producing cells. J Biol Chem 278:28346-53.

183. Lama J, Mangasarian A, Trono D. 1999. Cell-surface expression of CD4 reduces HIV-1 infectivity by blocking Env incorporation in a Nef- and Vpu-inhibitable manner. Curr Biol 9:622-31.

184. Levesque K, Finzi A, Binette J, Cohen EA. 2004. Role of CD4 receptor down-regulation during HIV-1 infection. Curr HIV Res 2:51-9.

185. Veillette M, Richard J, Pazgier M, Lewis GK, Parsons MS, Finzi A. 2016. Role of HIV-1 Envelope Glycoproteins Conformation and Accessory Proteins on ADCC Responses. Curr HIV Res 14:9-23.

186. Gohain N, Tolbert WD, Orlandi C, Richard J, Ding S, Chen X, Bonsor DA, Sundberg EJ, Lu W, Ray K, Finzi A, Lewis GK, Pazgier M. 2016. Molecular basis for epitope recognition by non-neutralizing anti-gp41 antibody F240. Sci Rep 6:36685.

187. Haim H, Si Z, Madani N, Wang L, Courter J, Princiotto A, Kassa A, DeGrace M,

bioRxiv preprint doi: https://doi.org/10.1101/2022.12.01.518799; this version posted December 2, 2022. The copyright holder for this preprint (which was not certified by peer review) is the author/funder, who has granted bioRxiv a license to display the preprint in perpetuity. It is made available under aCC-BY-NC-ND 4.0 International license.

McGee-Estrada K, Mefford M, Gabuzda D, Smith AB III, Sodroski J. 2009. Soluble CD4 and CD4-mimetic compounds inhibit HIV-1 infection by induction of a short-lived activated state. PLoS Pathogens 5:e1000360.

188. Madani N, Princiotto AM, Zhao C, Jahanbakhshsefidi F, Mertens M, Herschhorn A, Melillo B, Smith AB III, Sodroski J. 2017. Activation and inactivation of primary human immunodeficiency virus envelope glycoprotein trimers by CD4-mimetic compounds. J Virol 91:e01880-16.

189. Privalov PL. 1990. Cold denaturation of proteins. Crit Rev Biochem Mol Biol 25:281-305.

190. Tsai CJ, Maizel JV, Jr., Nussinov R. 2002. The hydrophobic effect: a new insight from cold denaturation and a two-state water structure. Crit Rev Biochem Mol Biol 37:55-69.

191. Lopez CF, Darst RK, Rossky PJ. 2008. Mechanistic elements of protein cold denaturation. J Phys Chem B 112:5961-7.

192. Sanders RW, Vesanen M, Schuelke N, Master A, Schiffner L, Kalyanaraman R, Paluch M, Berkhout B, Maddon PJ, Olson WC, Lu M, Moore JP. 2002. Stabilization of the soluble, cleaved, trimeric form of the envelope glycoprotein complex of human immunodeficiency virus type 1. J Virol 76:8875-89.

193. Sanders RW, Schiffner L, Master A, Kajumo F, Guo Y, Dragic T, Moore JP, Binley JM. 2000. Variable-loop-deleted variants of the human immunodeficiency virus type 1 envelope glycoprotein can be stabilized by an intermolecular disulfide bond between the gp120 and gp41 subunits. J Virol 74:5091-100.

194. Schulke N, Vesanen MS, Sanders RW, Zhu P, Lu M, Anselma DJ, Villa AR, Parren PW, Binley JM, Roux KH, Maddon PJ, Moore JP, Olson WC. 2002. Oligomeric and conformational properties of a proteolytically mature, disulfide-stabilized human immunodeficiency virus type 1 gp140 envelope glycoprotein. J Virol 76:7760-76.

195. Madani N, Princiotto AM, Schon A, LaLonde J, Feng Y, Freire E, Park J, Courter JR, Jones DM, Robinson J, Liao H-X, Moody MA, Permar S, Haynes B, Smith AB III, Wyatt R, Sodroski J. 2014. CD4-mimetic small molecules sensitize human immunodeficiency virus (HIV-1) to vaccine-elicited antibodies. J Virol 88:6542-6555.

196. Reed LJ, Muench H. 1938. A simple method of estimating fifty percent endpoints. Am J Hyg 27:493-97.

197. Ozanne G. Estimation of endpoints in biological systems. 1984. Comput Biol Med 14:377-84.

bioRxiv preprint doi: https://doi.org/10.1101/2022.12.01.518799; this version posted December 2, 2022. The copyright holder for this preprint (which was not certified by peer review) is the author/funder, who has granted bioRxiv a license to display the preprint in perpetuity. It is made available under aCC-BY-NC-ND 4.0 International license.

FIGURE LEGENDS

FIG 1 Comparison of virus pseudotypes and virions produced by an infectious molecular clone (IMC). (A) 293T cells and HeLa cells were transfected with the pSVIIIenv AD8 plasmid expressing the full-length HIV-1_{AD8} Env alone (AD8) or together with the pNL4-3.ΔEnv plasmid, or the pNL4-3.AD8 IMC alone (2 μg of each plasmid was used, whether alone or in combination). When the pSVIIIenv AD8 expressor plasmid was used, a plasmid expressing the HIV-1 Tat protein was also transfected at an 8:1 Env:Tat weight ratio. Forty-eight to seventy-two hours later, the cell supernatants were collected, filtered through a 0.45-μm membrane and centrifuged at 14,000 x g for 1 h at 4°C. In parallel, the cells were lysed. Precipitated particles and clarified cell lysates were Western blotted with a goat anti-gp120 antibody, the 4E10 anti-gp41 antibody, the rabbit anti-hsp70 antibody and the mouse anti-p24 serum. (B) 293T cells were transfected with the pSVIIIenv AD8 plasmid expressing the full-length HIV-1_{AD8} Env and the pNL4-3.ΔEnv plasmid at indicated weight ratios, or the pNL4-3.AD8 IMC alone. Cell lysates and virus particles were subsequently prepared and Western blotted as described above. (C) 293T cells and HeLa cells were transfected with the IMCs expressing the full-length AD8 Env, full-length Env with a defective cleavage site (−) or a truncated EnvΔ712 lacking the cytoplasmic tail. Cell lysates and virus particles were prepared and Western blotted as described above. The truncated form of gp41 in the Δ712 Env is indicated with an arrow. (D) 293T cells were transfected with the pNL4-3.AD8 IMC that is unmodified or modified with stop codons in the genes encoding reverse transcriptase (RT), RNAse H, integrase (IN), Vif, Vpr, Vpu or Nef. The cell lysates and virus particles were prepared and Western blotted as described above. Equal volumes of the clarified cell supernatants were used to infect TZM-bl cells for 48

bioRxiv preprint doi: https://doi.org/10.1101/2022.12.01.518799; this version posted December 2, 2022. The copyright holder for this preprint (which was not certified by peer review) is the author/funder, who has granted bioRxiv a license to display the preprint in perpetuity. It is made available under aCC-BY-NC-ND 4.0 International license.

hours, after which cells were lysed and the luciferase activity was measured. The results are representative of those obtained in two independent experiments, with the means and standard deviations reported. The full-length pNL4-3.AD8 IMC used in A-C encodes an AD8 Env with Bam (S752F I756F) changes in the cytoplasmic tail (see Fig. 3 below).

FIG 2 Characterization of the full-length AD8 Bam Env on IMC-produced virions. (A) 293T cells were transfected with the pNL4-3.AD8 IMC encoding an AD8 Env with Bam (S752F I756F) changes in the cytoplasmic tail (see Fig. 3 below). Forty-eight to seventy-two hours later, the cell supernatants were collected, filtered through a 0.45-μm membrane and centrifuged at 14,000-100,000 x g for 1 h at 4°C. Virus pellets were lysed, denatured and treated with PNGase F or Endo Hf for 1.5 h at 37°C, and Western blotted with a goat anti-gp120 antibody and the 4E10 anti-gp41 antibody. The deglycosylated (dg) Envs produced by PNGase F and Endo Hf are indicated by red and green labels, respectively. (B) Purified virus particles with AD8 Bam Envs were incubated with the BS3 crosslinker at the indicated concentrations for 30 min at room temperature. The samples were subsequently quenched, analyzed by reducing SDS-PAGE and Western blotted with a goat anti-gp120 antibody. (C) Purified virus particles were incubated with a panel of broadly neutralizing antibodies (bNAbs), poorly neutralizing antibodies (pNAbs) and the anti-HR1 C34-Ig peptide for 1 h at room temperature in the presence or absence of 10 μg/mL four-domain soluble CD4 (sCD4). The virus-antibody mixture was diluted twenty-fold with 1X PBS and centrifuged. The virus-antibody pellet was lysed and precipitated with Protein A-agarose beads for 1 h at

bioRxiv preprint doi: https://doi.org/10.1101/2022.12.01.518799; this version posted December 2, 2022. The copyright holder for this preprint (which was not certified by peer review) is the author/funder, who has granted bioRxiv a license to display the preprint in perpetuity. It is made available under aCC-BY-NC-ND 4.0 International license.

4°C. The beads were washed three times and Western blotted with a goat anti-gp120 antibody and the 4E10 anti-gp41 antibody. (D) Purified virus particles were incubated with 10 μM BMS-806 or with the indicated concentration of DTSSP crosslinker for 30 min at room temperature before the reactions were quenched with 100 mM Tris-HCl, pH 8.0. Env antigenicity on these virus particles was studied as described in (C). (E) 293T cells were transfected with the pNL4-3.AD8 Bam IMC expressing a soluble version of gp120. Forty-eight hours later, 0.45-μm filtered supernatant containing the soluble gp120 was crosslinked with 1 mM DTSSP as described above. Aliquots were then incubated with a panel of pNAbs and Protein A-agarose beads for 2 h at room temperature before the beads were washed and Western blotted with a goat anti-gp120 antibody. The results shown are representative of those obtained in two independent experiments. The means and standard deviations of the results in C and D are reported in the bar graphs in the panels on the right. The significance of the difference in antibody binding between treated and untreated samples was evaluated by a Student's t test; *, $p < 0.05$; **, $p < 0.01$.

FIG 3 Effects of cytoplasmic tail clipping on Env conformation. (A) 293T cells were transfected with the pNL4-3.AD8 or pNL4-3.AD8 Bam IMCs, the latter encoding the AD8 Env with Bam (S752F I756F) changes in the cytoplasmic tail. Forty-eight to seventy-two hours later, the cell lysates and virus particles were prepared and Western blotted as described in the Fig. 1A legend. Clipping of the gp41 subunit in the virus particles was reduced by the Bam changes. (B) Seventy-two hours after transfection of 293T cells with IMCs, the cell supernatants were collected, clarified with a soft spin and incubated for 1 h at 37°C with a panel of bNAbs and pNAbs, soluble CD4-Ig or the CD4-

bioRxiv preprint doi: https://doi.org/10.1101/2022.12.01.518799; this version posted December 2, 2022. The copyright holder for this preprint (which was not certified by peer review) is the author/funder, who has granted bioRxiv a license to display the preprint in perpetuity. It is made available under aCC-BY-NC-ND 4.0 International license.

mimetic compound BNM-III-170. The mixture was added to TZM-bl cells for 48 h, after which cells were lysed and the luciferase activity measured. The 50% inhibitory concentrations of the Env ligands are reported in μg/mL except for BNM-III-170 (in μM). (C) Antigenicity of the VLP AD8 Env with and without the Bam changes was analyzed as described in the Fig. 2C legend. The results are representative of those obtained in two independent experiments. The means and standard deviations of the results in B and C are reported in the bar graphs. The significance of the difference in antibody binding to the AD8 and AD8 Bam Envs in C was evaluated by a Student's t test; *, $p < 0.05$.

FIG 4 Effects of State-1-stabilizing and -destabilizing changes on virion Env. (A) Neutralization of the AD8 Bam and AD8 Bam 197 HT N viruses by the indicated Env ligands was measured as described in the Fig. 3B legend. The 50% inhibitory concentrations of the Env ligands are reported in μg/mL except for BNM-III-170 (in μM). (B) 293T cells were transfected with pNL4-3.env IMCs expressing the AD8 Bam Env, the State-1-destabilized AD8 Bam 197 HT N Env and the State-1-stabilized Envs Tri Bam and AE.1 Bam. Seventy-two hours later, virions were purified and the antigenicity of Env on virus particles was analyzed as described in the Fig. 2C legend. (C) 293T cells were transfected with the pNL4-3.env IMCs expressing soluble versions of gp120 (sgp120) from the indicated Envs. Forty-eight hours later, the cell supernatant containing secreted gp120 was collected, filtered through a 0.45 μm membrane and incubated with the indicated antibodies and Protein A-agarose beads for 2 h at room temperature. The beads were washed and Western blotted with a goat anti-gp120 antibody. (D) Purified virus particles were incubated with the crosslinker BS3 at the

bioRxiv preprint doi: https://doi.org/10.1101/2022.12.01.518799; this version posted December 2, 2022. The copyright holder for this preprint (which was not certified by peer review) is the author/funder, who has granted bioRxiv a license to display the preprint in perpetuity. It is made available under aCC-BY-NC-ND 4.0 International license.

indicated concentrations for 30 minutes at room temperature, after which the reactions were quenched and samples were analyzed by reducing SDS-PAGE and Western blotted with a goat anti-gp120 antibody. The results are representative of those obtained in two independent experiments. The means and standard deviations of the results in A and B are shown in the bar graphs. The significance of the difference in antibody binding between Env mutants and AD8 Bam Env was evaluated by a Student's t test; *, $p < 0.05$; **, $p < 0.01$; ***, $p < 0.001$.

FIG 5 Shedding of gp120 from Env on virus particles. (A) 293T cells were transfected with the pNL4-3.AD8 Bam plasmid. Forty-eight to seventy-two hours later, the cell supernatants were collected, filtered through a 0.45-μm membrane and centrifuged at 100,000 x g for 1 h at 4°C. Virus pellets were resuspended and incubated with four-domain soluble CD4 (sCD4) or the CD4-mimetic compound BNM-III-170 at the indicated concentrations and temperatures for 1 h. Virus particles were again pelleted and the supernatants containing shed gp120 were incubated with GNL beads for 2 h at room temperature. Beads were washed and Western blotted with a goat anti-gp120 antibody. The percentage of the gp120 Env on the input virus that was detected in the supernatants is plotted in the graphs on the right. (B) Shedding of gp120 from different Envs after a 1-h room temperature incubation with the indicated concentrations of BNM-III-170 was analyzed as described in A. (C) Purified virus particles were incubated at different temperatures for different lengths of time. Shed gp120 was then analyzed as described in A. (D) Purified virus particles with the AD8 Bam Env were incubated on ice in the presence of DMSO or 10 μM BMS-806 for different lengths of time. Shed gp120 was then analyzed as described in A. (E) Purified virus particles containing different

bioRxiv preprint doi: https://doi.org/10.1101/2022.12.01.518799; this version posted December 2, 2022. The copyright holder for this preprint (which was not certified by peer review) is the author/funder, who has granted bioRxiv a license to display the preprint in perpetuity. It is made available under aCC-BY-NC-ND 4.0 International license.

AD8 Env variants were incubated on ice for the indicated lengths of time and shed gp120 was then analyzed as described in A. Except for A, the results shown are representative of those obtained in two independent experiments. In B-D, the means and standard deviations are reported. The significance of the difference between DMSO- and BMS-806-treated samples (C) or between Tri Bam and AE.1 Bam Envs compared to AD8 Bam Env (D) was evaluated by a Student's t test; *, $p < 0.05$; **, $p < 0.01$; ***, $p < 0.001$.

FIG 6 Maintenance of Tri Bam Env antigenicity on virions after prolonged incubation on ice. HEK 293T cells were transfected with the pNL4-3.Tri Bam infectious molecular clone. Seventy-two hours later, virus particles were purified, aliquoted and stored at -80°C. Pilot experiments found no detectable difference in the Env content or antigenicity of VLPs that were analyzed directly after production or were frozen at -80°C once. One -80°C aliquot was thawed and incubated on ice for 7 days (+Ice). At this time, a second aliquot was thawed to serve as a reference control (−Ice). Both samples were pelleted and washed to remove any shed gp120, after which the Env antigenicity on virus particles was analyzed as described in the Fig. 2C legend. The results are representative of those obtained in two independent experiments, with the means and standard deviations reported in the bar graphs on the right.

FIG 7 Characterization of VLP Envs from other HIV-1 strains. (A) 293T cells were transfected with pNL4-3.env infectious molecular clones expressing the NL4-3, JR-FL E168K and BG505 Envs. Seventy-two hours later, virus particles were purified and Env antigenicity on virus particles was analyzed as described in the Fig. 2C legend. Note

bioRxiv preprint doi: https://doi.org/10.1101/2022.12.01.518799; this version posted December 2, 2022. The copyright holder for this preprint (which was not certified by peer review) is the author/funder, who has granted bioRxiv a license to display the preprint in perpetuity. It is made available under aCC-BY-NC-ND 4.0 International license.

2063 that in A only, the JR-FL E168K mutant was used to allow recognition by V2 quaternary
2064 bNAbs (PG16, PGT145) (147,148). The means and standard deviations of the results
2065 obtained in two independent experiments are reported in the bar graph at the right of
2066 the figure. The significance of the difference between AD8 Bam Env and other Envs
2067 was evaluated by a Student's t test; *, $p < 0.05$; **, $p < 0.01$; NA, not applicable. (B) The
2068 antigenicity of soluble gp120 versions of the indicated Envs was performed as
2069 described in the Fig. 4C legend. (C) The susceptibility of VLP Envs to gp120 shedding
2070 induced by BNM-III-170 or ice incubation was evaluated as described in the Fig. 5B and
2071 5E legend. (D) Env glycoprotein expression, processing and incorporation into virus
2072 particles were examined as described in the Fig. 1A legend. The results are
2073 representative of those obtained in at least two independent experiments.
2074
2075 **FIG 8** Characterization of Envs on virus particles from infected T cells. (A) HEK 293T
2076 cells were transfected with pNL4-3.env infectious molecular clones expressing the
2077 Strep-tagged AD8 Bam or E.1 Bam Envs. Addition of the Strep tag to the Env C
2078 terminus does not affect neutralization sensitivity nor Env antigenicity on virus particles
2079 (data not shown). Seventy-two hours later, the cell supernatants were clarified and ID_{50}
2080 values were determined using TZM-bl target cells. C8166-R5 cells were then infected
2081 with virus particles at a multiplicity of infection of 0.1. Cells were washed 5-16 h after
2082 infection and resuspended in fresh medium. Fresh medium was supplemented at three
2083 days after infection. Six to seven days after infection, virus particles were collected,
2084 purified and Env antigenicity was analyzed as described in the Fig. 2C legend. (B)
2085 293T cells were transfected with the pNL4-3.E.1 Bam Strep infectious molecular clone
2086 with or without a CD4-expressing plasmid at a 1:0.1 weight ratio. Seventy-two hours

bioRxiv preprint doi: https://doi.org/10.1101/2022.12.01.518799; this version posted December 2, 2022. The copyright holder for this preprint (which was not certified by peer review) is the author/funder, who has granted bioRxiv a license to display the preprint in perpetuity. It is made available under aCC-BY-NC-ND 4.0 International license.

later, virus particles were collected, purified and Env antigenicity was analyzed as described in the Fig. 2C legend. The results are representative of those obtained in at least two independent experiments. The means and standard deviations of the results from A and B are reported in the bar graphs (right panels). The significance of the difference between the wild-type AD8 Bam Env and E.1 Bam Env (A) or between VLP Envs made in the absence or presence of CD4 (B) was evaluated by a Student's t test; *, $p < 0.05$; ***, $p < 0.001$.

FIG 9 Model of Env conformations on virus particles. (A) Three populations of cleaved Env trimers on virus particles are depicted along with their distinguishing properties. Uncleaved (gp160) Env trimers, which are found to various extents on VLP preparations, are shown on the right. (B) The relative levels of cleaved Env trimer populations on virions are depicted for HIV-1 Envs with different levels of triggerability. The approximate relationship of the different HIV-1 Env variants used in this study is shown. Env triggerability is inversely related to the activation barrier separating State 1 from States 2/3 and varies among Envs from different primary HIV-1 strains (107). Envs with intermediate levels of triggerability, like the AD8 Bam Env, populate the pretriggered (State-1) conformation and also spontaneously sample more open, downstream (States 2/3) conformations. Viral Envs with lower triggerability (e.g., the Tri Bam or E.1 Bam Envs) populate the pretriggered (State-1) conformation on the virions to a greater extent. Conversely, viral Envs with higher triggerability (e.g., the AD8 Bam 197 HT N Env) exhibit more open trimer conformations on the virions and are more prone to shed gp120, leading to gp41-only trimers. (C) Modulation of virion Env conformational transitions. Upon binding to membrane CD4 on a target cell, the

bioRxiv preprint doi: https://doi.org/10.1101/2022.12.01.518799; this version posted December 2, 2022. The copyright holder for this preprint (which was not certified by peer review) is the author/funder, who has granted bioRxiv a license to display the preprint in perpetuity. It is made available under aCC-BY-NC-ND 4.0 International license.

pretriggered (State-1) Env conformation undergoes transitions to more open (State-2/3) intermediates in which the gp120 coreceptor-binding site is exposed. Env binding to the CCR5 or CXCR4 coreceptor promotes additional conformational changes in Env that facilitate virus entry (green arrows). Depending on its triggerability, HIV-1 Env will spontaneously sample more open (State-2/3) conformations (curved black arrow) in which epitopes for some pNAbs become exposed. Such spontaneous transitions from State 1 can be suppressed by State-1-stabilizing Env changes or by treatment of the Env trimers with BMS-806 or chemical crosslinkers (red minus sign). Conversely, State-1-destabilizing Env changes or treatment with sCD4 or CD4-mimetic compounds (CD4mcs) drive Env trimers out of State 1 and increase the level of virion Envs in more open conformations (green plus sign). When in close proximity to a potential target cell expressing CCR5 or CXCR4 coreceptors, virions with Envs in these open (State-2/3) conformations can infect the cell (168,169,171,187,188). However, compared with Envs that engage CD4 on a target membrane, Envs opened by other means are more prone to either spontaneous inactivation or neutralization by pNAbs (36,49,187,188,195). The pNAb-reactive, open Env intermediates exhibit weak intersubunit interactions compared to the bNAb-reactive State-1 Env trimers. Certain HIV-1 isolates like HIV-1_{AD8} are not neutralized by pNAbs yet show pNAb binding to cleaved Env on virus particles; this apparent paradox can be resolved if the cleaved Env recognized by pNAbs is partially or completely dysfunctional. Our results suggest that gp120 shedding is more likely to occur from more open Env conformers (red arrow).

bioRxiv preprint doi: https://doi.org/10.1101/2022.12.01.518799; this version posted December 2, 2022. The copyright holder for this preprint (which was not certified by peer review) is the author/funder, who has granted bioRxiv a license to display the preprint in perpetuity. It is made available under aCC-BY-NC-ND 4.0 International license.

Fig 1

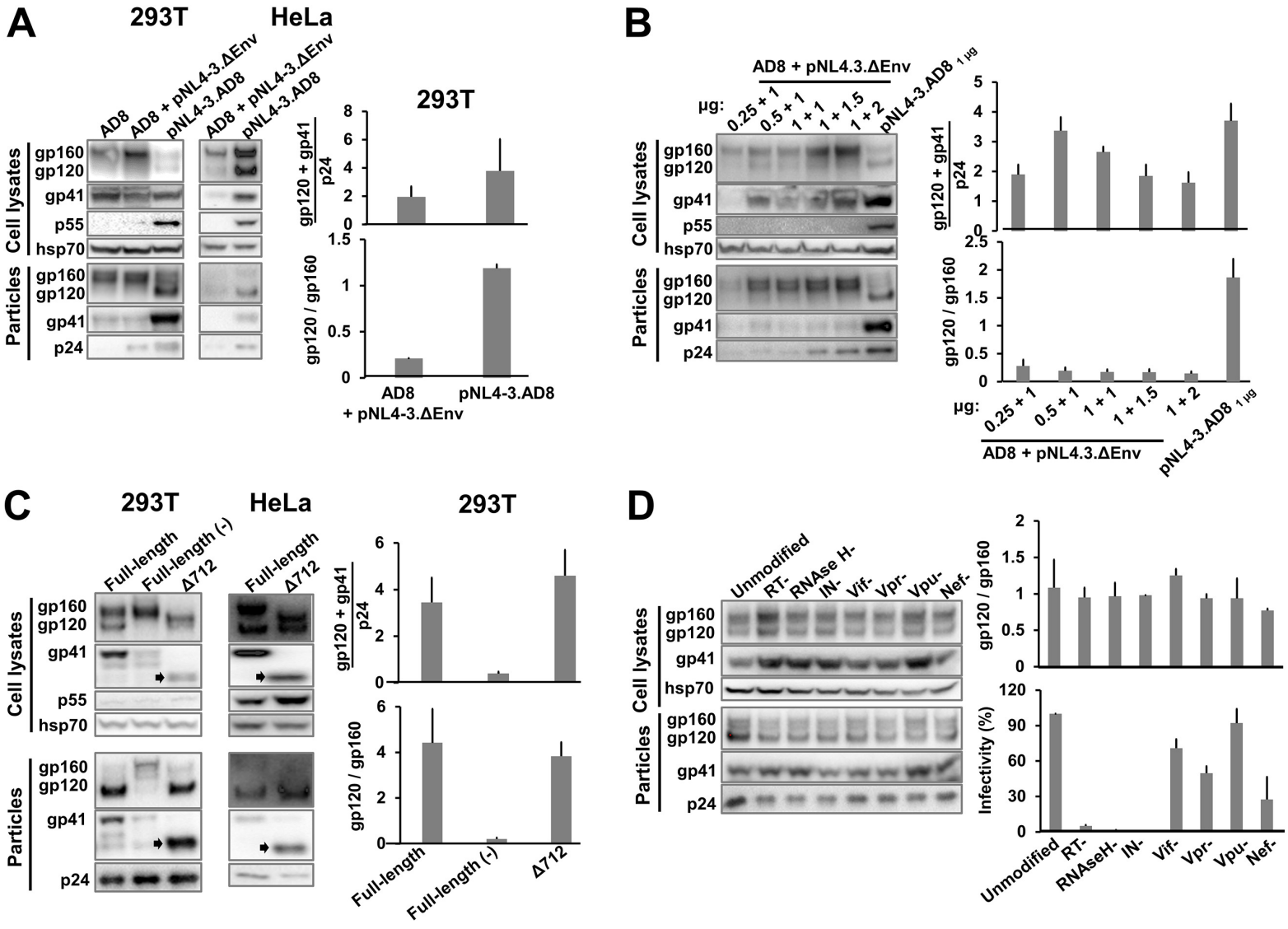

bioRxiv preprint doi: https://doi.org/10.1101/2022.12.01.518799; this version posted December 2, 2022. The copyright holder for this preprint (which was not certified by peer review) is the author/funder, who has granted bioRxiv a license to display the preprint in perpetuity. It is made available under aCC-BY-NC-ND 4.0 International license.

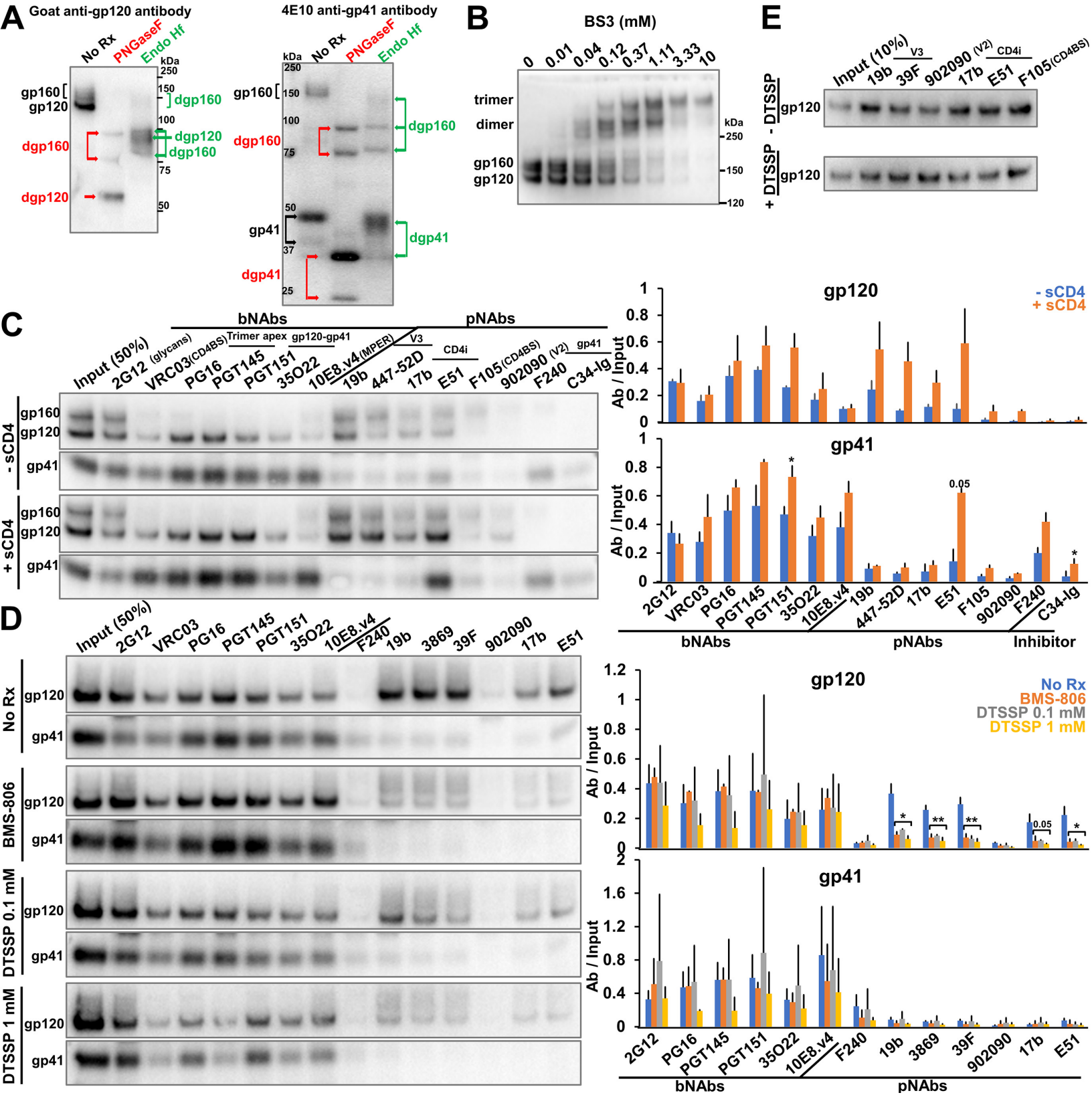

bioRxiv preprint doi: https://doi.org/10.1101/2022.12.01.518799; this version posted December 2, 2022. The copyright holder for this preprint (which was not certified by peer review) is the author/funder, who has granted bioRxiv a license to display the preprint in perpetuity. It is made available under aCC-BY-NC-ND 4.0 International license.

Fig 3

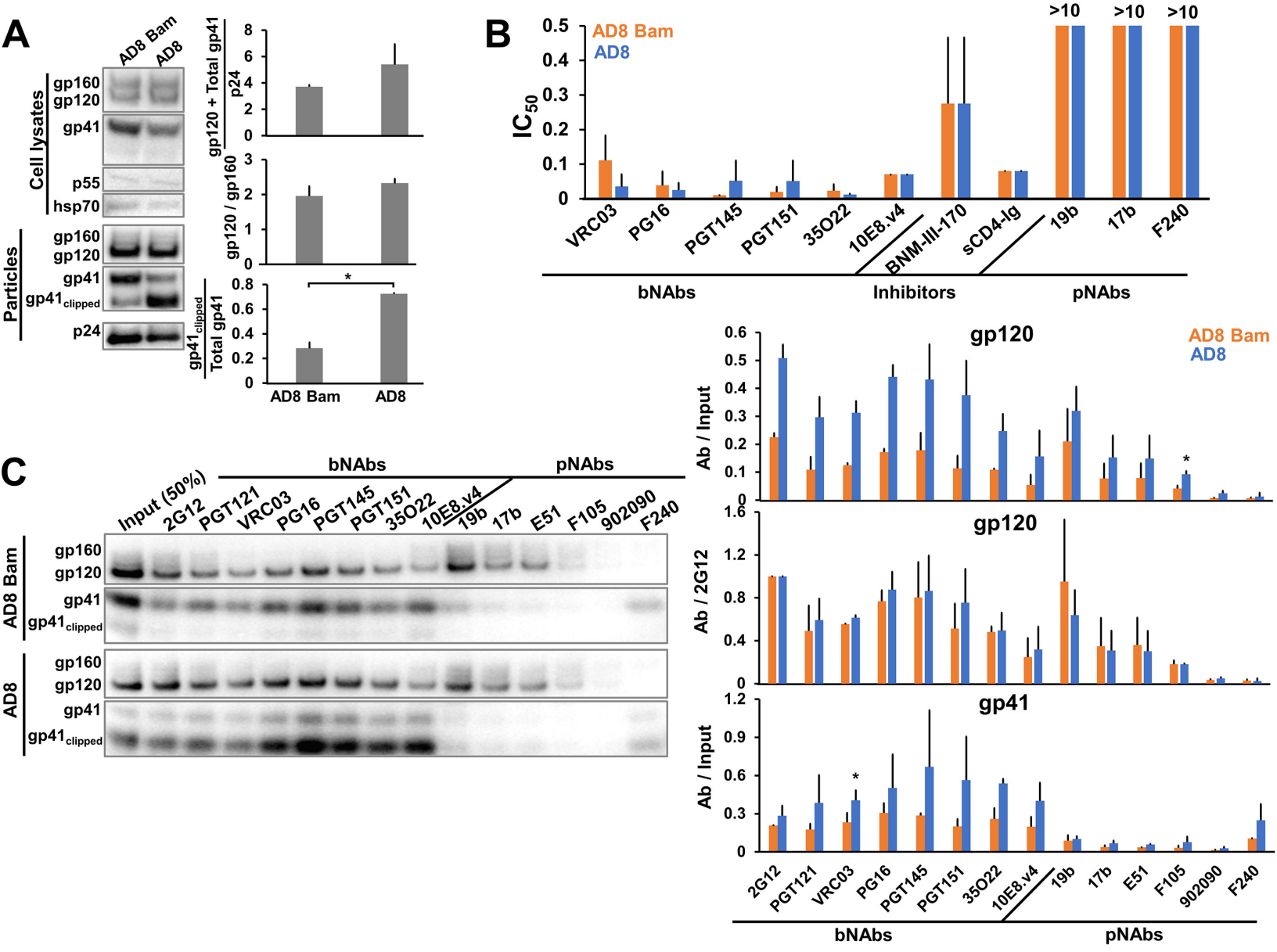

bioRxiv preprint doi: https://doi.org/10.1101/2022.12.01.518799; this version posted December 2, 2022. The copyright holder for this preprint (which was not certified by peer review) is the author/funder, who has granted bioRxiv a license to display the preprint in perpetuity. It is made available under aCC-BY-NC-ND 4.0 International license.

Fig 4

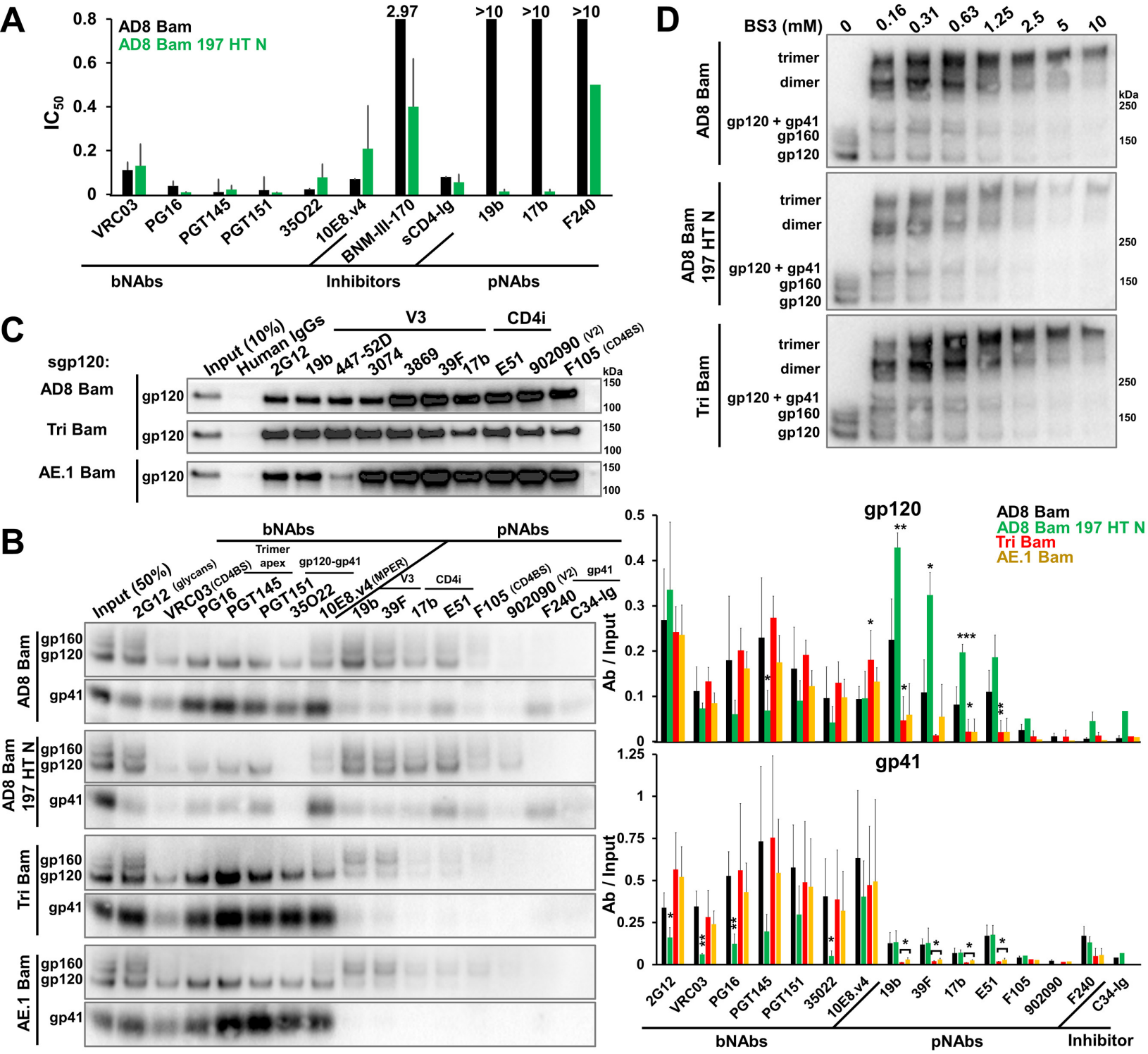

bioRxiv preprint doi: https://doi.org/10.1101/2022.12.01.518799; this version posted December 2, 2022. The copyright holder for this preprint (which was not certified by peer review) is the author/funder, who has granted bioRxiv a license to display the preprint in perpetuity. It is made available under aCC-BY-NC-ND 4.0 International license.

Fig 5

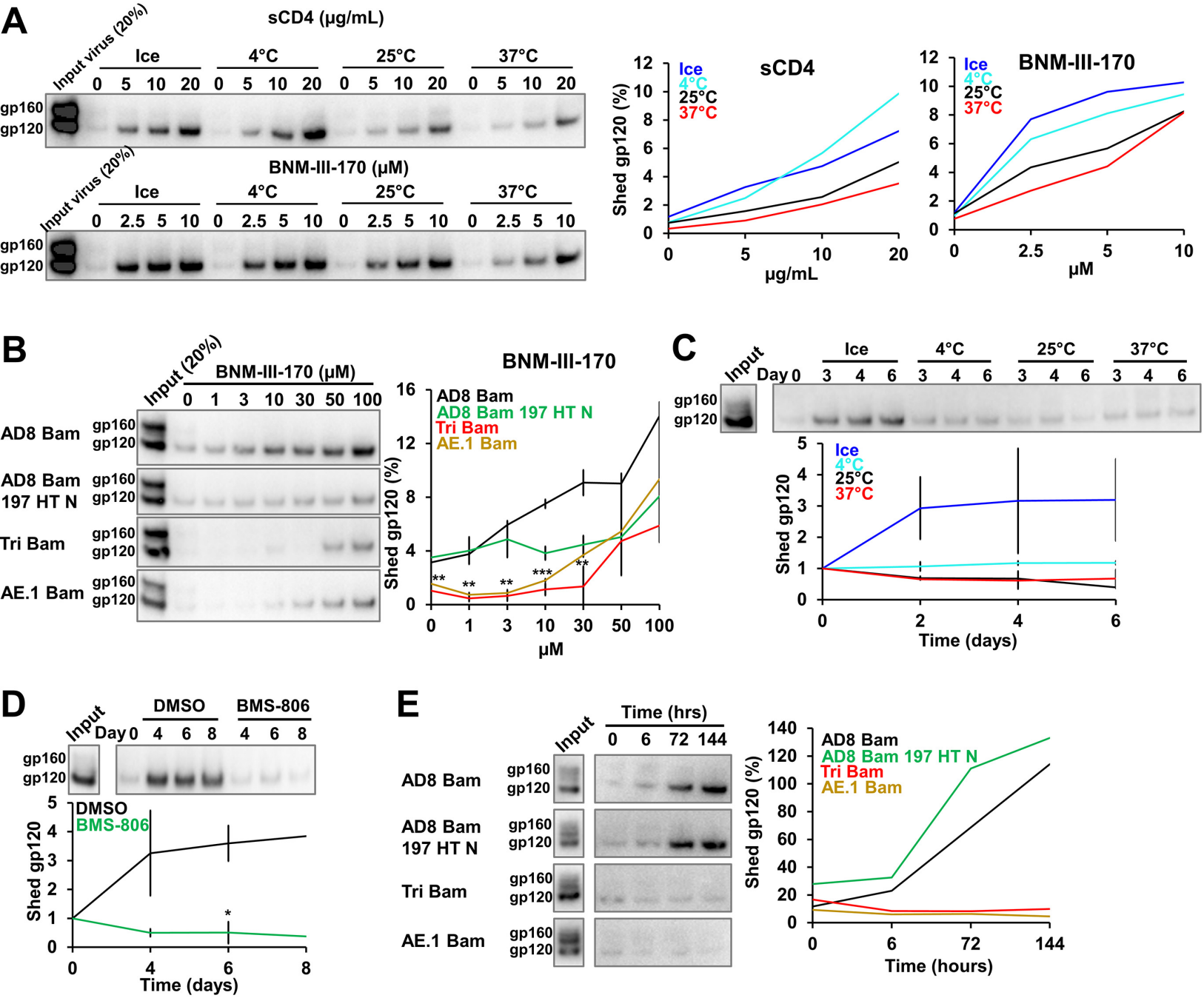

bioRxiv preprint doi: https://doi.org/10.1101/2022.12.01.518799; this version posted December 2, 2022. The copyright holder for this preprint (which was not certified by peer review) is the author/funder, who has granted bioRxiv a license to display the preprint in perpetuity. It is made available under aCC-BY-NC-ND 4.0 International license.

Fig 6

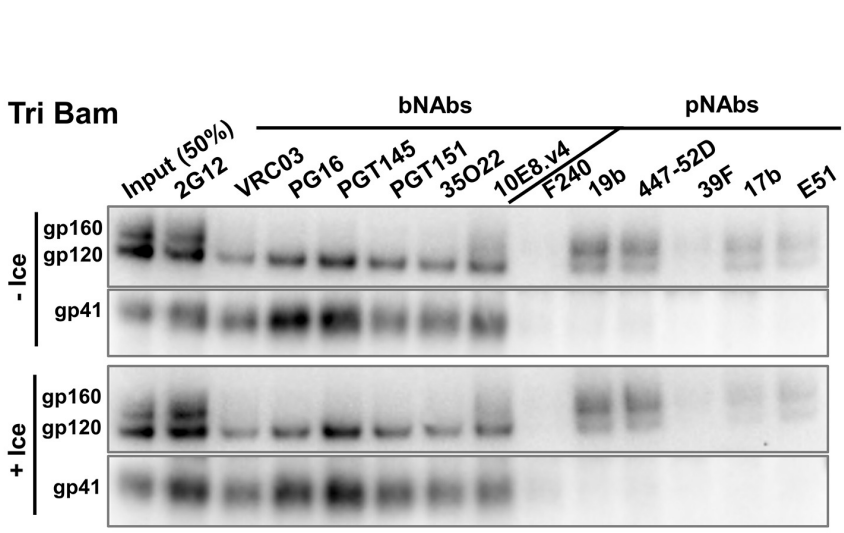

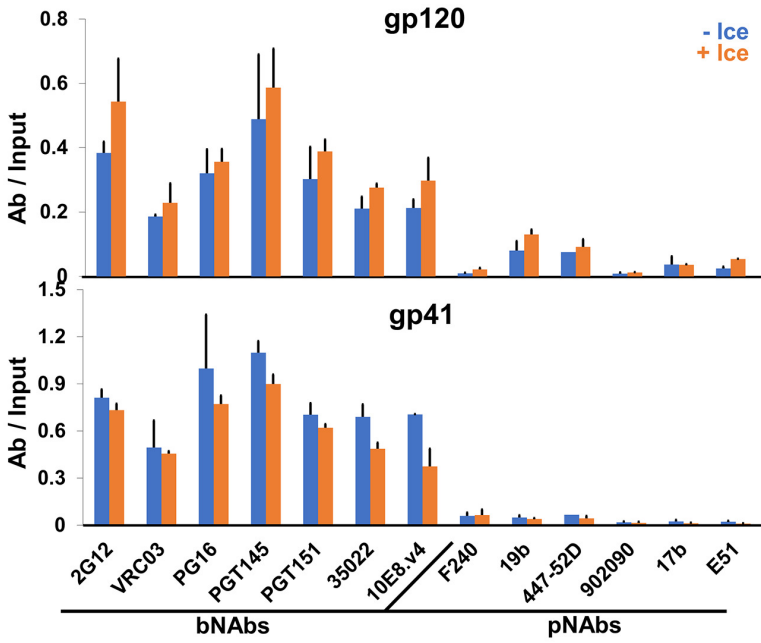

bioRxiv preprint doi: https://doi.org/10.1101/2022.12.01.518799; this version posted December 2, 2022. The copyright holder for this preprint (which was not certified by peer review) is the author/funder, who has granted bioRxiv a license to display the preprint in perpetuity. It is made available under aCC-BY-NC-ND 4.0 International license.

Fig 7

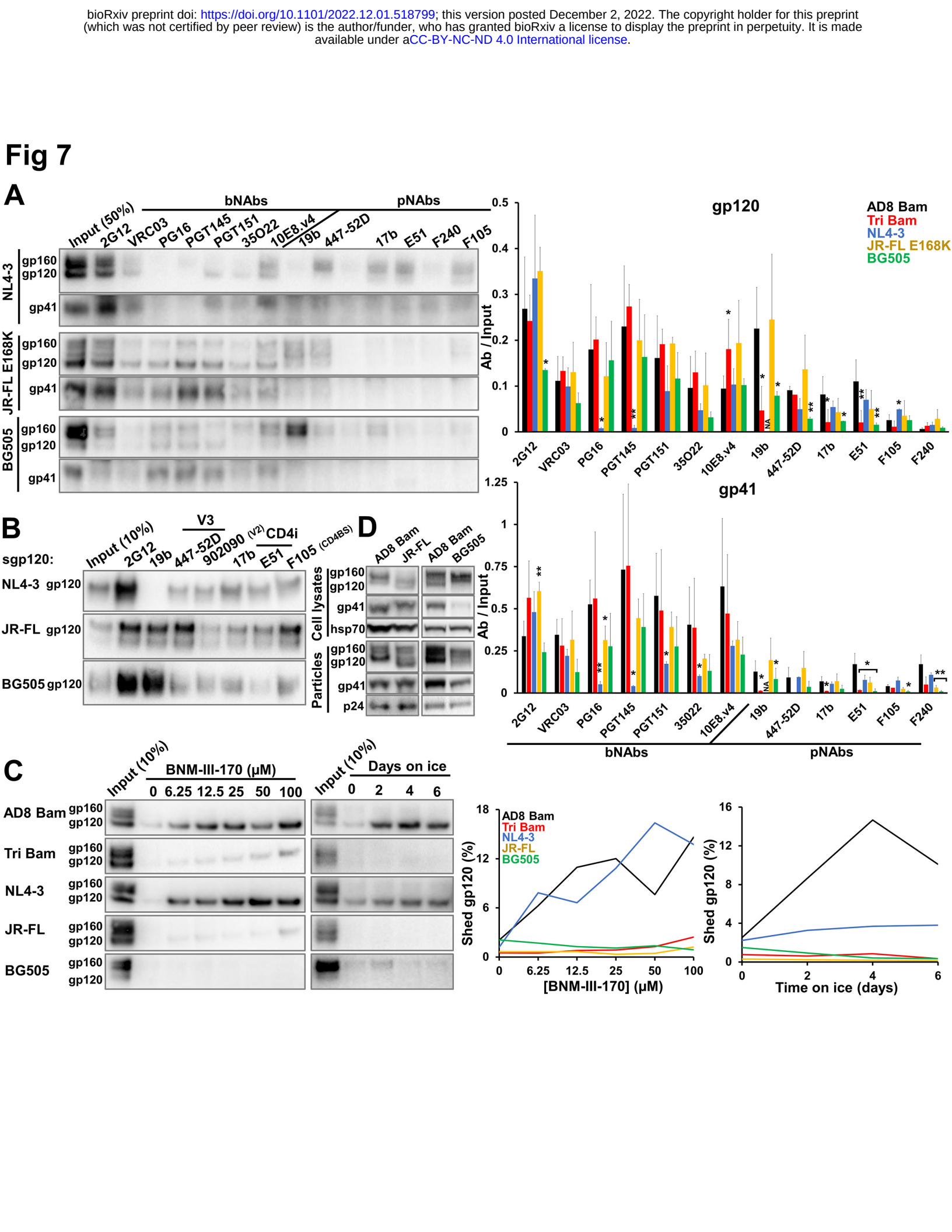

bioRxiv preprint doi: https://doi.org/10.1101/2022.12.01.518799; this version posted December 2, 2022. The copyright holder for this preprint (which was not certified by peer review) is the author/funder, who has granted bioRxiv a license to display the preprint in perpetuity. It is made available under aCC-BY-NC-ND 4.0 International license.

Fig 8

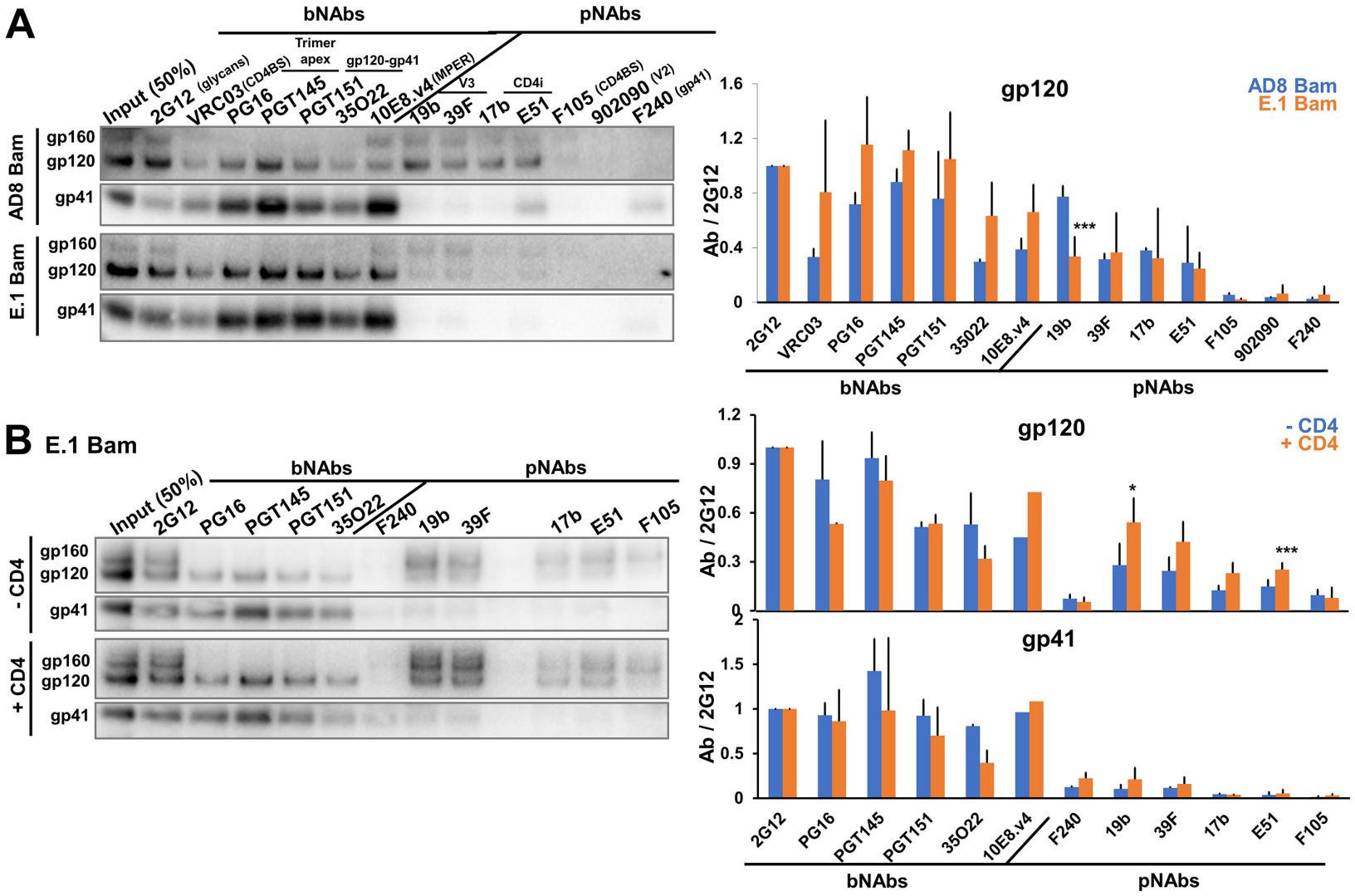

bioRxiv preprint doi: https://doi.org/10.1101/2022.12.01.518799; this version posted December 2, 2022. The copyright holder for this preprint (which was not certified by peer review) is the author/funder, who has granted bioRxiv a license to display the preprint in perpetuity. It is made available under aCC-BY-NC-ND 4.0 International license.

Fig 9